D2.5 Local air quality models with fuel compositional effects

Date: October, 2024

Funded by
the European Union

This Project has received funding from the European Union's HORIZON Research and Innovation Programme under Grant Agreement number 101096698

Document Identification			
Status	Final	**Due Date**	31/01/2026
Version	1.0	**Submission Date**	19/03/2025

Related WP	WP2.5	**Document Reference**	D2.5
Related Deliverable(s)	N/A	**Dissemination Level (*)**	PU
Lead Participant	TUD	**Lead Author**	Luccas K. Kavabata, Irene C. Dedoussi
Contributors	UC3M, UoB, KTH, S&T	**Reviewers**	Gerardo Zampino, KTH
			Hakki Aksoy, KTH

Keywords:
aircraft emissions, air quality, sustainable aviation fuels

Document Information

List of Contributors	
Name	**Partner**
Simon Blakey	University of Birmingham
Hakki Aksoy	KTH
Evelyn Otero Sola	KTH
Luccas Koji Kavabata	TU Delft
Irene Dedoussi	TU Delft & University of Cambridge
Frank Hogervorst	S[&]T
Edo Loenen	S[&]T

Document History			
Version	**Date**	**Change editors**	**Changes**
0.1	15/01/2025	Luccas Koji Kavabata	Writing the first draft
0.2	30/01/2025	Luccas Koji Kavabata	Writing the review of the deliverable
1.0	10/03/2025	Luccas Koji Kavabata	Final version

Quality Control		
Role	**Who (Partner short name)**	**Approval Date**
Deliverable leader	Irene Dedoussi (TUD)	10/03/2025
Quality manager	Gerardo Zampino (KTH)	19/03/2025
Project Coordinator	Ricardo Vinuesa (KTH)	19/03/2025

Table of Contents

1. Introduction 7
1.1. Purpose of the document 7
1.2. Structure of the document 7
2. Emissions modelling 8
2.1. Existing datasets, engine certification and conventional fuels 9
2.2. Combustion simulations (UoB) 10
2.2.1. Combustor design 10
2.2.2. Fuel Chemistry 11
2.2.3. Combustor modeling 13
2.2.4. Gaseous emissions 16
2.2.5. Particulate matter emissions 17
2.3. Aviation emissions calculation (KTH) 21
2.3.1. Calculation of EIs for HC, CO and NOX 22
2.3.2. Calculation of EI for Non-Volatile Particulate Matter (nvPM) 27
2.3.3. Calculation of Fuel Properties and fuel composition-based EIs 31
3. Air quality modelling 35
3.1. Atmospheric chemistry transport modelling (TUD) 35
3.1.1. Introduction 35
3.1.2. Objectives 36
3.1.3. Methods 36
3.1.4. LTO attributable air quality effects 38
3.1.5. Next steps 40
3.2. Observational approach (S&T) 40
4. Conclusions 45

List of Tables

Table 2.1 - Fuel specific information reported in ICAO EEDB

Table 2.2 - Jet Fuel Surrogates from the literature (composition in mole fractions, y_i) for conventional jet fuel

Table 2.3 - Available kinetic models

Table 2.4 - Species of interest from REFMAP project

Table 2.5 - Fuel property table

Table 3.1 - user needs for air quality monitoring in the vicinity of airports

Table 3.2 - derived user requirements air quality in the vicinity of airports

List of Figures

Figure 2.1 - Interaction and information flow between consortium members in WP2.5.

Figure 2.2 - Chemical classification of Jet Fuel composition [1].

Figure 2.3 - Figure 2.3 - Aeronet model (2003) [2].

Figure 2.4 - Calculated unburnt hydrocarbon emissions results for CFM56-5B engines with SAC combustor.

Figure 2.5 - Calculated CO emissions results for CFM56-5B engines with SAC combustor.

Figure 2.6 - Calculated NOx emissions results for CFM56-5B engines with SAC combustor.

Figure 2.7 – Combined data for IAE V2500 floatwall engines from EEBD showing the change in nvPM number and mass across the operating thrust of the aircraft.

Figure 2.8 - nvPM mass for IAE V2500 floatwall engine across operating range.

Figure 2.9 - nvPM number for IAE V2500 floatwall engine across operating range.

Figure 2.10 - nvPM mass at mid power condition (42kN) vs fuel composition.

Figure 2.11 - nvPM number at mid power condition (42kN) vs fuel composition.

Figure 2.12 - nvPM number at high power condition (96kN) vs fuel composition.

Figure 2.13 - nvPM number at high power condition (96kN) vs fuel composition.

Figure 2.14 - Process of the proposed SAF-modified BFFM2.

Figure 2.15 - The flow chart of MEEM method for conventional fuels (numbered in black) and SAF blends (numbered in red).

Figure 2.16 - Figure 2.12 - Average properties chart for conventional fuels and synthetic fuels [3].

Figure 3.1 - Stretched cubed-sphere grid based on a C24 grid resolution used for the simulations.

Figure 3.2 - LTO attributable annual-averaged mass of black carbon aerosol in gC.m-3 (left) and $PM_{2.5}$ in g.cm-3 (right) in Europe at ground level.

Figure 3.3 - LTO attributable annual-averaged NO2 (left) and O_3 concentration in Europe in ppbv at surface level.

Figure 3.4 - Overview of observational approach for producing air quality maps.

List of Acronyms

Abbreviation / acronym	Description
ACARE	Advisory Council for Aviation Research and Innovation
ARP	Aerospace Recommended Practice
ATM	Air Traffic Management
BFFM2	Boeing Fuel Flow Method 2
CA	Certifying authority
CAMS	Copernicus Atmospheric Monitoring Service
CFD	Computational Fluid Dynamics
CO	Carbon monoxide
CO_2	Carbon dioxide
CORSIA	Carbon Offsetting and Reduction Scheme for International Aviation
CRECK	Chemical Reaction Engineering and Chemical Kinetics Lab
CRN	Chemical Reactor Network
D2.5	Deliverable number 2.5 belonging to WP2.5
EASA	European Union Aviation Safety Agency
EC	European Commission
EEDB	Engine Emissions Data Base
EI	Emissions indices
ESA	European Space Agency
ETS	Emissions Trading Scheme
FOA	Fiber Optic Association
GCHP	GEOS-Chem High Performance
IAE	International Aero Engines
ICAO	International Civil Aviation Organization
LHV	Lower Heat Value
LTO	Landing and take-off operations
MRV	Monitoring, Recording and Ultimately
MTF	Mixed Turbo Fan
NO	Nitrogen oxides
NO	Nitric oxide
NO_2	Nitrogen dioxide
NO_x	Nitrogen oxides
nvPM	Non-volatile particulate matter
O_3	Ozone
OEMs	Original Engine Manufacturers
OpenAVEM	Open Aviation Emissions Model
P3T3	Ratio or reference methods

PFR	Plug Flow Reactor
PM	Particulate matter
PSR	Perfectly Stirred Reactor
REFMAP	Reducing the environmental impact of air travel
S2F2	Sustainable Supersonic Fuel Flow Method
SAC	Southern Auto Castings
SAE	Society of Automotive Engineers
SAF	Sustainable aviation fuels
SN	Smoke number
UHC	Unburnt hydrocarbons
WP	Work Package

Executive Summary

The Task T2.5 aims to address the local impact of air traffic on air quality in the proximity of airports taking into account fuel compositional effects. The research into this topic involves the modelling of emissions, which includes investigating the products of different types of fuel combustion, e.g., kerosene, sustainable aviation fuels (SAF), SAF blends; the differences in the aircraft exhaust species due to different types of aircraft engines; calculation of the emission indices of the exhaust species with sufficient degree of accuracy, and air quality modelling, which evaluates the dispersion, chemical reactions, and concentrations maps of the combustion products once they are exhausted from aircraft engines at different scales, e.g., local scale (city or country) or global scale (world-wide effects).

This deliverable aims to provide the reader an overview of the research activities that have been performed by Task T2.5. More specifically, it provides a detailed description of combustion simulations using different fuels types, the estimation of aviation emissions indices for various exhaust species, evaluating Landing and Take-off operations (LTO) impacts on local air quality, and an development of observational approach.

Task T2.5 has been developing a framework for simulating aircraft fuel combustion for different fuel types, the calculation of the emissions indices of aircraft exhaust products, the simulation of the dispersion of these species in the atmosphere, and the development of concentration maps based on the observational approach.

The next steps of Task T2.5 should include the analysis of different SAF blends, e.g., the combustion of SAF, their emissions indices, etc, and how they may help mitigate the impacts of aviation emissions on local air quality, especially near airports.

1. Introduction

1.1. Purpose of the document

The objective of this document is to provide a clear and concise overview of the activities being developed by Task T2.5 on local air quality models with fuel compositional effects. Each partner has contributed to this document by detailing the on-going research, including results obtained up to this point, as well as the next steps to be taken.

1.2. Structure of the document

This document is structured in 3 major chapters.

Chapter 2 presents the research efforts of the University of Birmingham and KTH and their work on combustion simulation and aviation emissions calculation, respectively.

Chapter 3 provides the research conducted by TU Delft and S&T on atmospheric chemistry modelling and the observational approach, respectively.

Chapter 4 includes the conclusions of Task T2.5 as of the time of the writing of the present report.

2. Emissions modelling

Assessment of the impact of aviation on the environment requires an agreed framework for the Monitoring, Recording and ultimately Verification (MRV) of aircraft attributable emissions. In the absence of direct and continuous measurements, a protocol is needed to calculate the emissions impact of particular flights and has been well established in the European airspace by EUROCONTROL [4] and initially used to compute the amount of fuel used in Europe.

As the development of MRV protocols for the reporting of climate impact of aviation emerge, the EUROCONTROL method is being questioned and expanded to include gaseous and particulate matter metrics, ultimately for the purpose of the planned Emissions Trading Scheme (ETS) within Europe [5] and the International Civil Aviation organization (ICAO)'s Carbon Offsetting and Reduction Scheme for international Aviation (CORSIA) [6]. Importantly, the EU ETS is planning on including non-CO_2 emissions, whereas CORSIA will not include these emissions.

In parallel, a number of academically driven research projects are developing protocols and procedures to perform Air Traffic Management (ATM) optimisation to minimise environmental impact of all flights in a particular airspace. REFMAP is one of these projects, looking forward to provide optimisation tools to account for environmental emissions, including traditional gaseous emissions, particulate matter (for the formation of non-CO_2 related climate impacts and for local air quality) and noise.

Of particular importance is the ability to predict the impact of Sustainable Aviation Fuels (SAFs) on the likely optimised ATM and flight trajectories. Whilst generally, the overall emissions from a flight may be minimised by flying the route with a minimum fuel burn. It has been shown that flights avoiding particular climate sensitive regions, may have a lower overall environmental impact while burning more fuel from a SAF source.

This is particularly challenging, as sufficient SAF fuel volumes are not available to carry out this assessment using real-time measured data or using the empirical approaches laid out in [4]. A new approach is required to achieve the goal of estimating SAF impacts at a fleet wide level. In the REFMAP project, the team will take up the challenge using a chemical kinetic modelling approach used in earlier work published by the team at Birmingham [7].

Birmingham University is contributing to the activities in Task T2.5, focusing on gaseous and particulate matter emissions. The overall interaction between the work in Birmingham and the wider work of Task T2.5 is laid out in Figure 2.1.

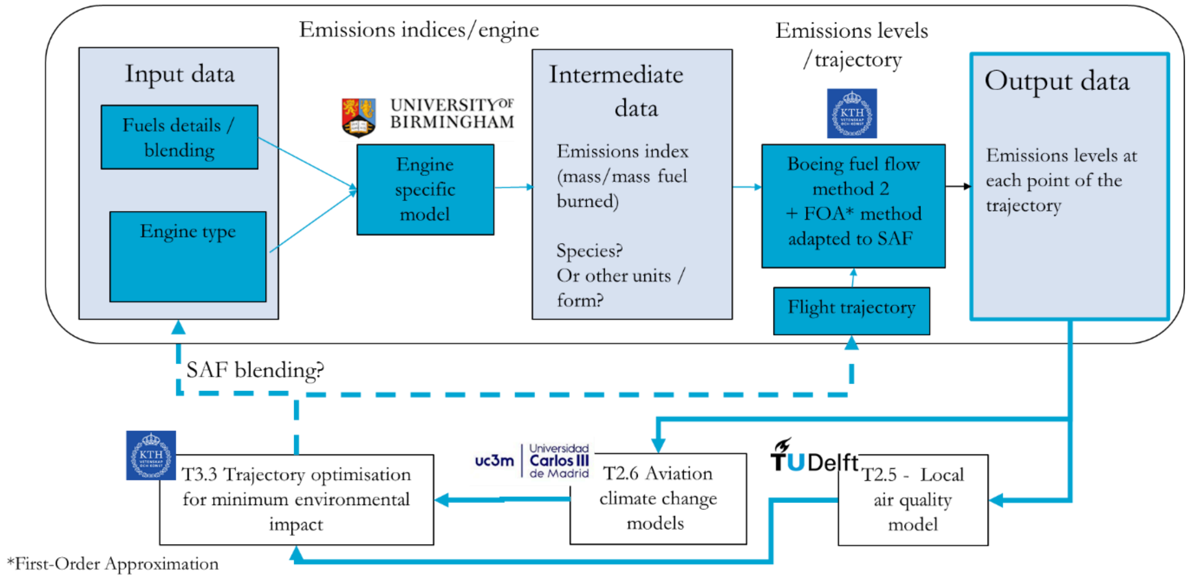

Figure 2.1 - Interaction and information flow between consortium members in WP2.5

It can be seen from figure 2.1, that the input data for the air quality model, i.e., the SAF blend ratio and engine type, is analysed by the University of Birmingham, who then provides engine specific emissions data for conventional fuels and blends with SAFs in the form of emissions indices (intermediate data) to KTH.

These emissions indices are then processed by KTH to obtain trajectory specific emissions, by using the Boeing fuel flow method 2 and FOA method adapted to SAF (figure 2.1). The results obtained by KTH are the outputs of the air quality research, which are then fed into TU Delft and UC3M.

TU Delft takes the output data to run atmospheric chemistry model GEOS-Chem High-Performance (GCHP) to produce yearly averaged maps of chemical species of concern to air quality, such as NO_X, O_3, and $PM_{2.5}$, and to assess mortality rates attributable to aircraft emissions. UC3M uses the outputs of the air quality research to evaluate the aviation climate change models.

Finally, the data from air quality and climate change models are fed into KTH, so that trajectory optimisation can be performed with the goal of minimising the environmental impact of aviation.

2.1. Existing datasets, engine certification and conventional fuels

Original Engine Manufacturers (OEMs) submit ground-based emissions data for all engines with a static thrust over 26.7kN to the primary certifying authority (CA) for approval as part of the engine certification process. The data is gathered on the exhaust emissions of production aircraft engines in the engine emissions data base

(EEDB) measured to the procedures in ICAO Annex 16, Volume II and hosted by the European Union Aviation Safety Agency (EASA) on behalf of ICAO as an open source dataset [8].

At the time of writing this document, the ICAO database version is 29B. It is anticipated that the dataset be updated at least annually as OEMs present updated data on engines produced. The data gathered on gaseous emissions (carbon monoxide (CO), nitrous oxides (NOx), unburnt hydrocarbons (UHC) and smoke number (SN)) should be compliant with the SAE ARP standards 1256E, 1179D and 1533D at the time of writing. In 2020 the requirements around the recording of particulate matter (PM) were changed to take account for improved measurement methods. All metrics are recorded at four engine test points at 100%, 85% 30% and 7% of maximum thrust, indicating take off (T/O), climb out (C/O), approach (App) and idle (Idle) conditions respectively.

The gaseous emissions and smoke data for each engine are reported in the form of an emissions index (EI) which is the mass of emission produced per unit mass of fuel burnt (typically, the reporting units are g/kg) along with the fuel flow rate. Table 2.1 shows the emissions indices and fuel composition information.

Table 2.1 – Fuel specific information reported in ICAO EEDB

	Gaseous emissions and smoke to SAE ARP 1256E	Non-volatile particulate matter SAE ARP 6320A
Fuel specification	report	report
H/C ratio	report min and max	
Aromatic content (%vol)	report min and max	report
Calorific value (MJ/kg)		report
Hydrogen content (%mass)		report
Naphthalene content (%mass)		report
Sulphur content (%mass)		report

Table 2.1 contains many of the key fuel parameters which are considered in the literature to dominate the fuel emission, particularly the non-volatile PM (nvPM) dataset. Unfortunately, the gaseous emissions and smoke test data for specific engines do not necessarily correspond to the same, which makes reading between datasets a challenging task, given that the data may not be entirely compatible.

2.2. Combustion simulations (UoB)

2.2.1. Combustor design

Gas turbine derivative engines are currently the primary providers of thrust for modern aircraft and have been developed since the late 1950s for civil aviation. The efficiency of these engines has been increasing since this time period, and consequently the fuel burn per unit thrust provided (or specific fuel consumption, *sfc*) has decreased.

In parallel to the obvious requirement for higher efficiencies and reduced fuel burn, regulating bodies such as the Advisory Council for Aviation Research and Innovation (ACARE) are putting increasingly stringent targets on the emissions from aircraft engines. The ACARE Flightpath 2050 targets are for a 75% reduction in CO_2 emissions, a 90% reduction in NOx and a 65% reduction in aircraft noise.

The efficiency of a gas turbine is determined by the detailed thermodynamic cycle of the gas turbine engine design. In other words, the higher the temperature and pressure of the core flow into the combustor, the higher the overall efficiency of the cycle. Where producing high levels of thrust for low fuel consumption are most important, the high bypass ratio engine has been widely adopted as the most efficient design of turbomachine.

The combustor entry temperature and pressures are not normally provided in the EEDB and will need to be estimated using thermodynamic models of the engine cycles; this is the so-called P3T3 approach, indicating the pressure and temperature of the flow at the combustor entry. However, it is worth noting that the other significant unknown variable is the air flow through the combustor.

2.2.2. Fuel Chemistry

2.2.2.1. Real fuel

The chemistry of conventional and SAF fuels is made up of thousands of components and is too complex to model completely. The species can be grouped into classes as indicated in Figure 2.2, in order to make the chemistry understandable. However this is computationally too expensive to assess directly and model, and so surrogate fuels are used to predict combustion and emissions performance in model work.

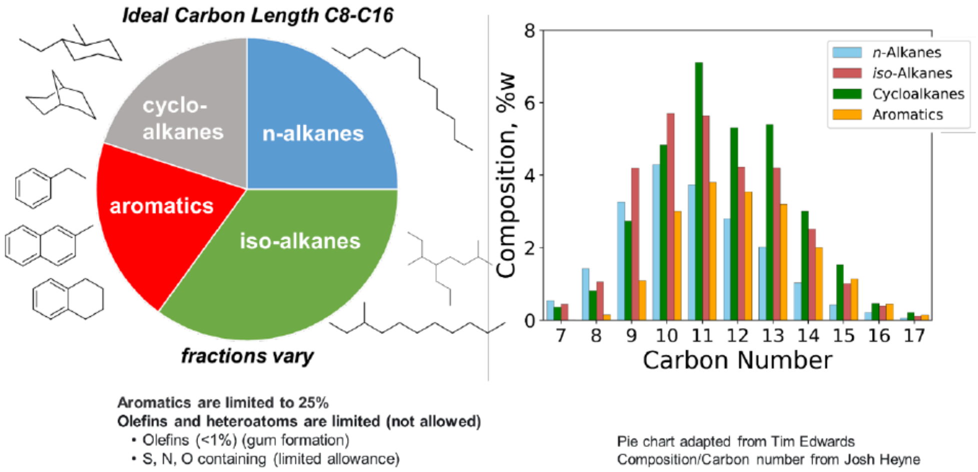

Figure 2.2 - Chemical classification of Jet Fuel composition [1].

2.2.2.2. Model surrogate fuel

The fuel composition used for kinetic modelling has evolved over time. Early studies tended to reduce fuel to n-dodecane and toluene as a surrogate for jet fuel. More recent studies have incorporated a more representative chemistry, and the various reported approaches are presented in Table 2.2.

Table 2.2 – Jet Fuel Surrogates from the literature (composition in mole fractions, y_i) for conventional jet fuel

	S0 [7]	S1 [9]	S2 [10]	S3 [11]	S4 [11]	S5 [12]
Species						
n-dodecane	0.890	0.404	0.303	0.384	0.290	0.371
Iso-octane		0.295				0.020
1,3,5- trimethylbenzene		0.073				
n-propyl benzene		0.228				
methylcyclohexane			0.485	0.234		
m-xylene			0.212			
Iso-cetane				0.148	0.142	0.206
toluene	0.110			0.234	0.249	0.259
decalin					0.319	0.145
naphthalene		0.020	0.020	0.020	0.020	0.020

It is important to note that with the exception of S0, most of these surrogates have been designed for the prediction of fuel properties, particularly auto-ignition delay.

2.2.3. Combustor modelling

A complete understanding of the emissions generated by a particular (albeit a surrogate) fuel in a particular combustor with a particular engine setting presents a considerable challenge to modelling techniques. If a detailed understanding of the combustor geometry is obtainable it is possible to develop computational fluid dynamics (CFD) models to address this, although often the fuel chemistry and reaction mechanisms are simplified. An alternative approach is to retain a high level of fidelity in the kinetic model but sacrifice some of the geometry features and use a chemical reactor network (CRN) to approximate the chemical mixing going on in the combustion chamber. This approach is more relevant for REFMAP as relatively simple networks can be developed and modelled with different fuel compositions to predict the impact of changes in fuel chemistry on specific combustor and engine performance.

A PSR network or a hybrid PSR-PFR (plug flow reactor) network can be commonly used to simulate mixing and flow characteristics of a gas turbine combustor [13-14]. This reactor network approach can significantly reduce the computational burden yet provide reasonable solutions for a complicated combustion process. However, constructing such a reactor network is rather empirical. Slight changes in combustor operating conditions often lead to a new reactor network configuration with a different number of reactors and connectivity. Typically, a gas turbine reactor network consists of a flame/ignition zone, a recirculation zone, and a post-flame zone. However, depending on how the fuel and oxidizer are delivered and the complexity of the flow field, additional reactors and inlets may be needed to properly represent the combustor.

Research carried out by the AERONET project suggested that aerospace combustors could be modelled as a complex combination of reactors as shown in Figure 2.3 [2] or as a linear series of greater than 5 perfectly stirred reactors (PSRs). For the Task T2.5, a network of 10 reactors split into two parallel paths will be used to replicate the fast and slow reacting species in the combustor [15].

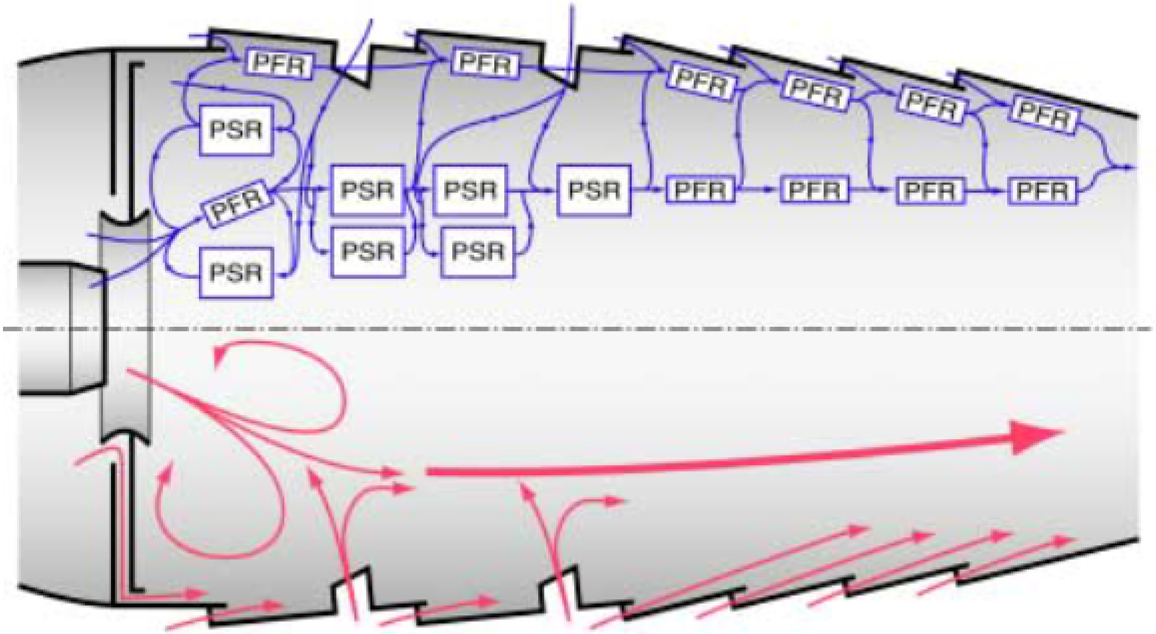

Figure 2.3 - Aeronet model (2003) [2].

A number of chemical kinetic models to replicate the combustion process are presented in Table 2.3. These models are increasingly complex, and offer an arguably more detailed description of the likely chemical composition of the exit gases, although at an increased computational cost. For this deliverable, the AFRMv2.1 model was used and compared to the CRECK Detailed model.

Table 2.3 - Available kinetic models

Name	Date	Species	Reactions
AFRMv2.1	2005	320	852
CRECK Reduced v1410	2014	121	2613
HyChem NTC A2	2018	130	995
CRECK Detailed v2003 HT_SOOT_NOX	2020	497	24501

Closer collaboration with TUD has resulted in a list of “species of interest” to be drawn up for further analysis in Table 2.4. The chemical kinetic model used in this deliverable is able to predict these species. It seems no model available includes sulphur chemistry, except for some of the AFRMv2.1 versions. For this study, a new kinetic model has been developed, taking the 115 reaction, 21 species sulphur model from AFRM and adding it to a CRECK yaml code.

Table 2.4 - Species of interest from REFMAP project

Species of interest from REFMAP community	Comments
NOX (NO, NO2) SOX CO Organic carbon (hydrophilic) Acetone Methacrolein Acetaldehyde Formaldehyde Lumped aldehyde >= C3 Sulfur dioxide Sulfate Black carbon Glyoxal Methylglyoxal Methanol Phenol SOAP Hydrocarbons Lumped >= C4 alkanes Ethane Propane Lumped >= C3 alkenes Black carbon (hydrophilic) Benzene Ethylene Acetylene Naphthalene Toluene Xylene	Not in standard mechanisms (see note below) Not able to distinguish between this and carbon Not in standard mechanisms (see note below) Not in standard mechanisms (see note below) Not in any mechanism (dialdehyde OCHCHO) Not in any mechanism (CH_3CCHO) Secondary Organic Aerosol Formation Potential?

2.2.4. Gaseous emissions

The licence for the flight modelling software used by UC3M is for an Airbus A320 with a CFM56-5B4/P SAC engine. This has been the primary engine modelled by the emissions analysis. The dataset produced from the modelling is EI emissions with variable thrust and variable SAF percentage. This creates a 3D array of data which is shared with KTH as a *.csv* file. A subset of the data is presented in the figures below.

The majority of the SAF and nvPM data for comparison with SAF is from the APEXII programme, which used a CFM56-2C1 engine model. The CFM56-2C1 also used a

SAC combustor and a CFM56-2C1 engine model was used with the SAC combustor to validate the combustor model, and then the combustor model was used in the CFM56-5B model to generate a dataset for incorporating into the KTH and UC3M models.

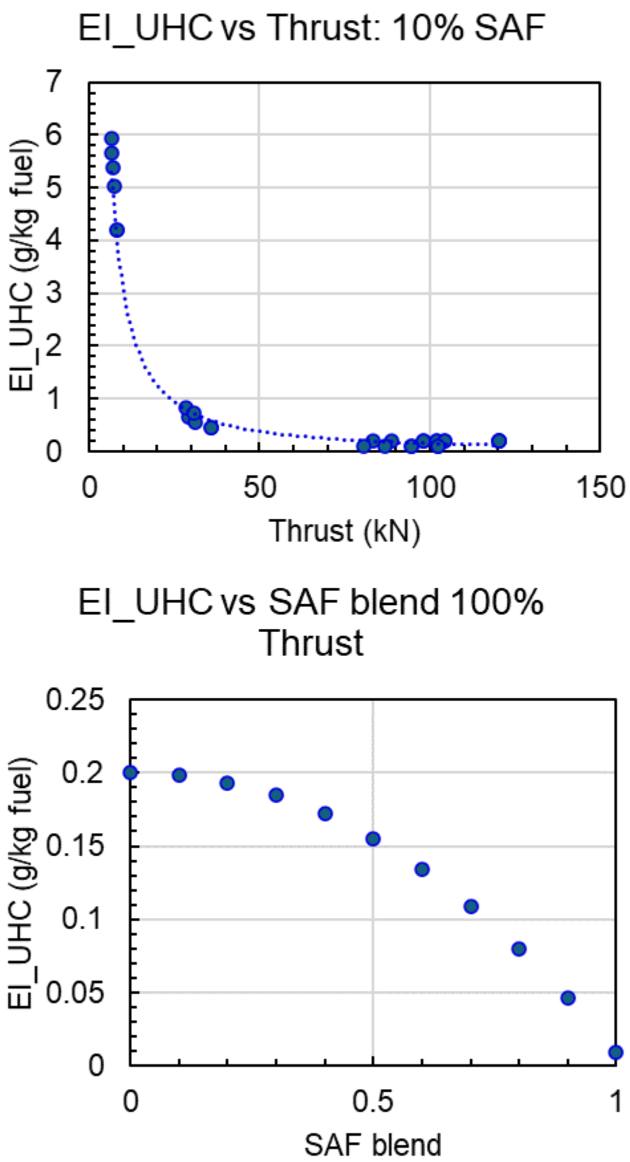

Figure 2.4 - Calculated unburnt hydrocarbon emissions results for CFM56-5B engines with SAC combustor

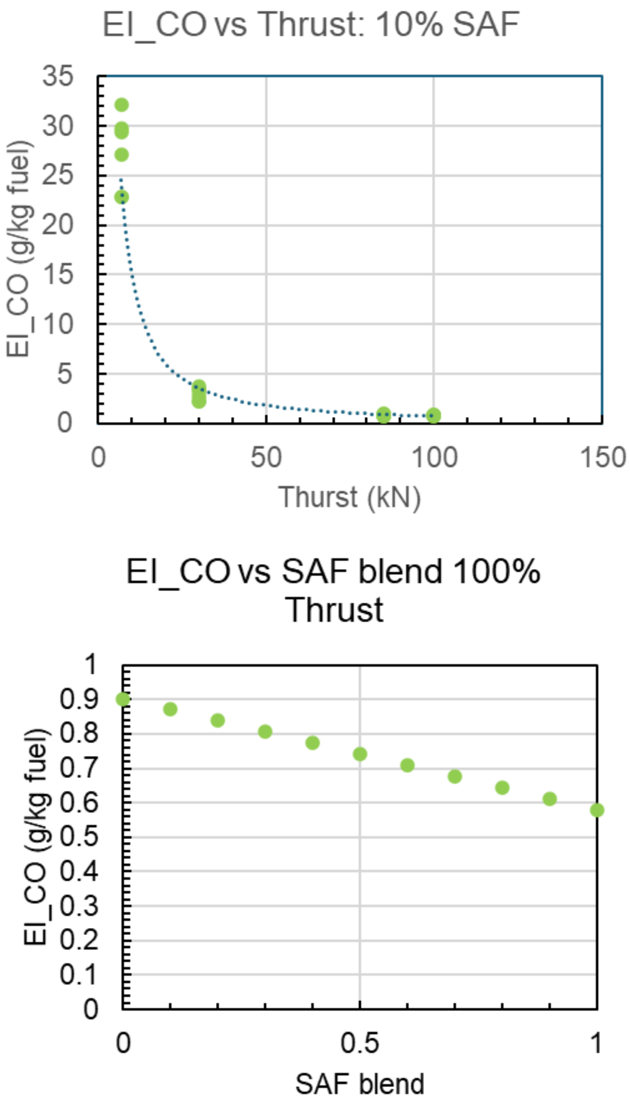

Figure 2.5 - Calculated CO emissions results for CFM56-5B engines with SAC combustor.

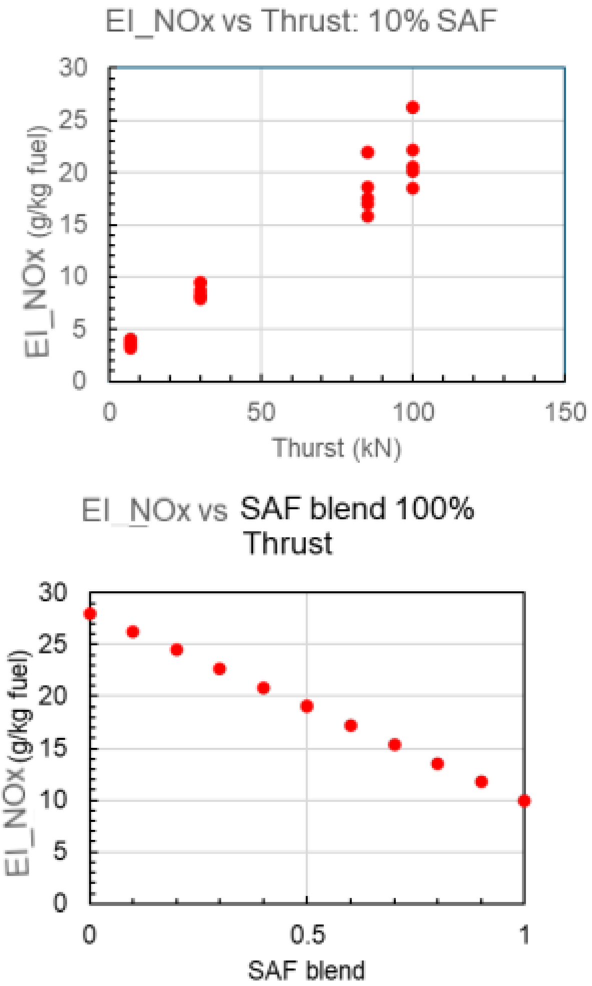

Figure 2.6 - Calculated NOx emissions results for CFM56-5B engines with SAC combustor

2.2.5. Particulate matter emissions

The modelling of particulate matter emissions to the same level of accuracy as the gaseous emissions is a challenging task. Active research is going on in the area in order to overcome the difficulties involved in obtaining more accurate estimates of particulate matter emissions.

A semi-empirical approach has been proposed in the REFMAP project to collate the information available in the public domain and produce correlations of particulate matter emission as a function of fuel composition. This work takes advantage of the research studies carried out on SAF performance in the limited flight tests conducted so far and combining this with the available data for conventional fuels from the EEBD. This is limited by the availability of research data for the engines of interest.

This work has been carried out on the IAE V2500 engine class with a floatwall combustor. The available data for this engine from the EEBD is provided in figure 2.7
.

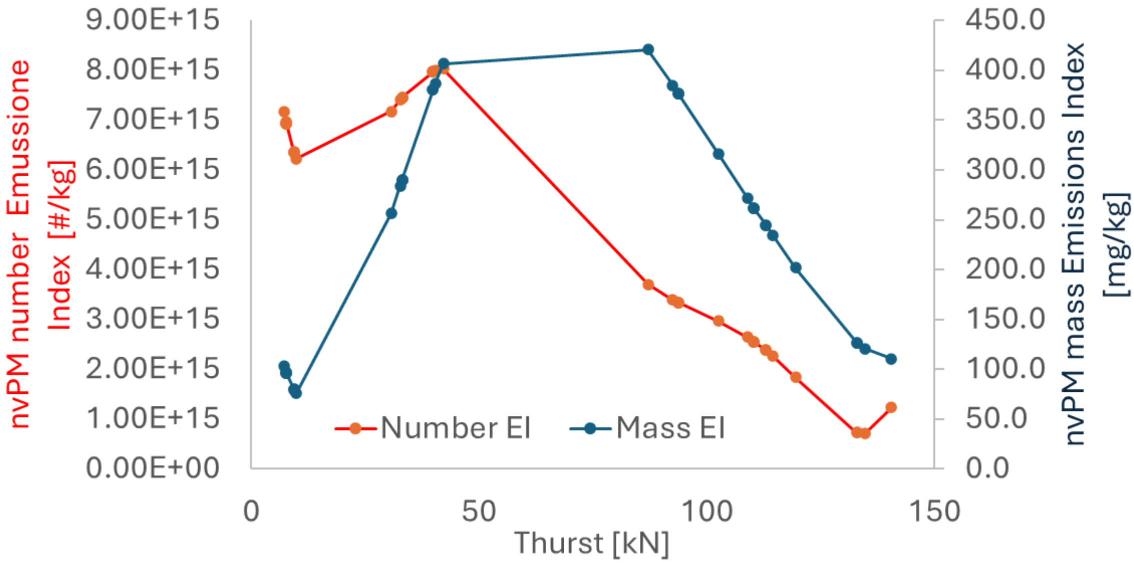

Figure 2.7 - combined data for IAE V2500 floatwall engines from EEBD showing the change in nvPM number and mass across the operating thrust of the aircraft.

The composition of fuel impacts directly on the nvPM emissions produced. A summary of the available data and fuel chemistry is presented in Table 2.5.

Table 2.5 - Fuel property table

Full Description	Vol%	Mixed (vol%)	Test fuel	100% Jet A1 (Merox)	100% Jet A1 ("Bitumen run")	100% FSJF	59% Ref 1 + 41% SPK	55% Ref 2 + 45% SPK	86% Ref 1 + 14% SPK
Heat of combustion	kJ/kg	ASTM D240	43.22	42.8	43.2	43.33	43.496	43.56	43.301
Smoke point	mm	ASTM D1322	N/A	25	26	25	26	26	25
Density at 15^oC	kg/m^3	ASTM D4052	N/A	812.7	808.9	807.9	790.2	783.4	803.2
Aromatics	Vol%	ASTM D1319	16.6	18.8	17.2	8.9	11.4	10.9	15.3
Naphthalene	Vol%	ASTM D1840	2.38	1.51	1.83	0	0.82		
Sulphur content	% by mass	ASTM D2622	0.054	0.117	0.135	0	0.057	0.07	0.159
C	Mass %	ASTM D5291	N/A	84.8	85.5	85		84	85
H	Mass %	ASTM D5291	13.83	14.1	14.1	14.5	14.36	14.7	14.2
H/C ratio	Mass %			1.922	1.925	1.981	2.029	2.045	1.954

Figures 2.8 and 2.9 show the same data combined with available data from SAF research testing. The data shows a clear reduction in nvPM mass compared to

conventional fuel as the blend percentage and type of SAF increase. The data for nvPM numbers is less clear.

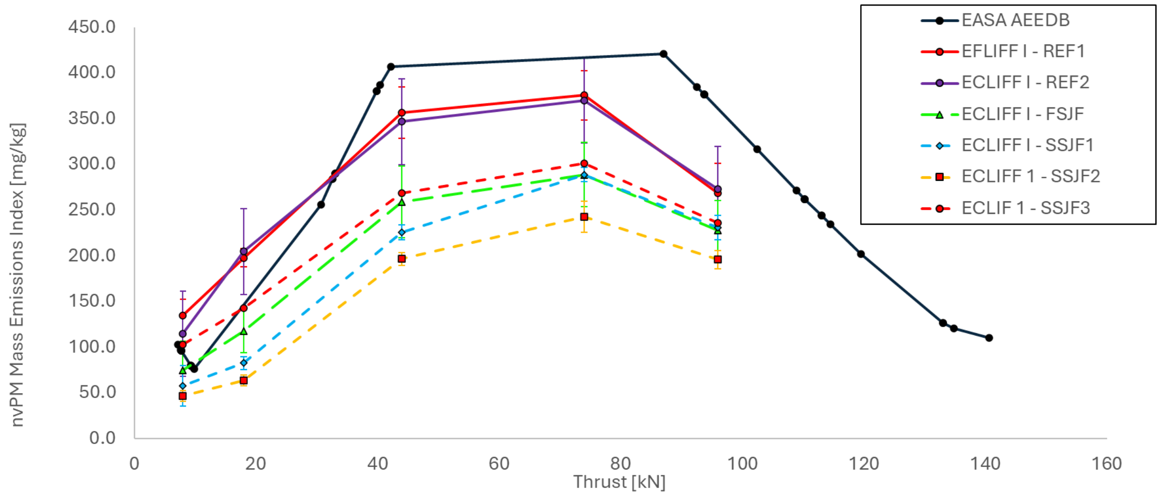

Figure 2.8 - nvPM mass for IAE V2500 floatwall engine across operating range

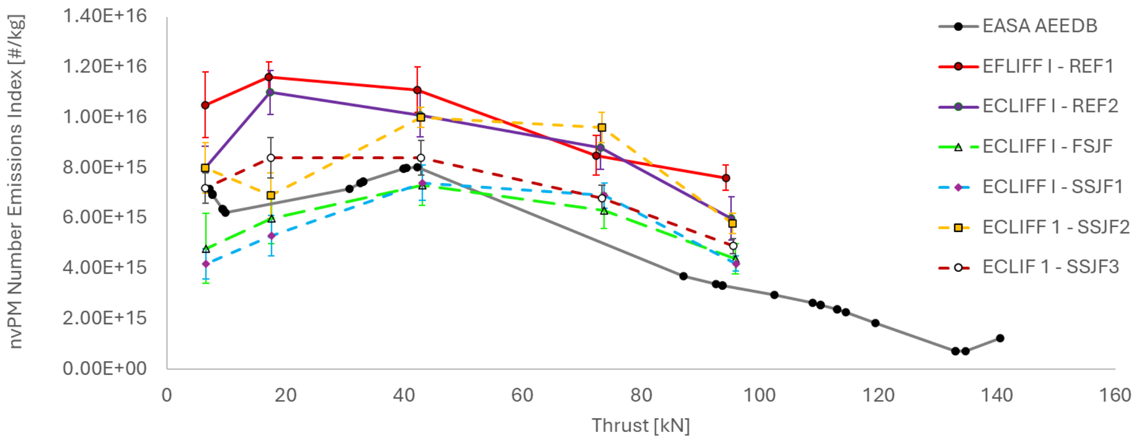

Figure 2.9 - nvPM number for IAE V2500 floatwall engine across operating range

Comparisons against fuel composition have been made at two operating conditions. Firstly a high power condition (96kN) and a mid-power condition (42kN). At these conditions, the mass and number concentrations are plotted against Naphthalene, total aromatic, total sulphur and hydrogen content.

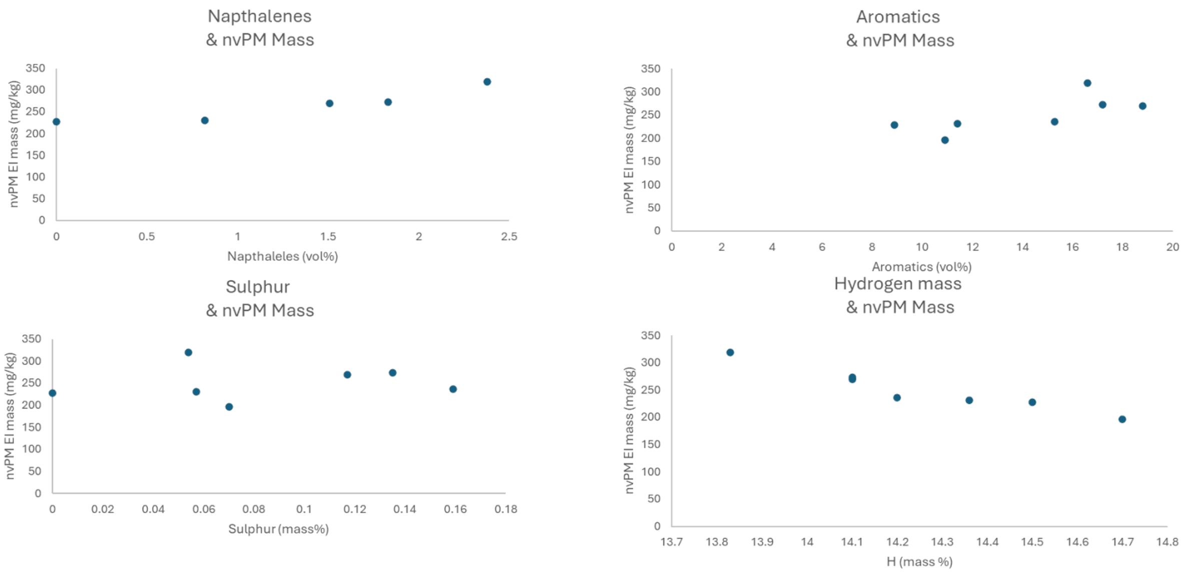

Figure 2.10 - nvPM mass at mid power condition (42kN) vs fuel composition

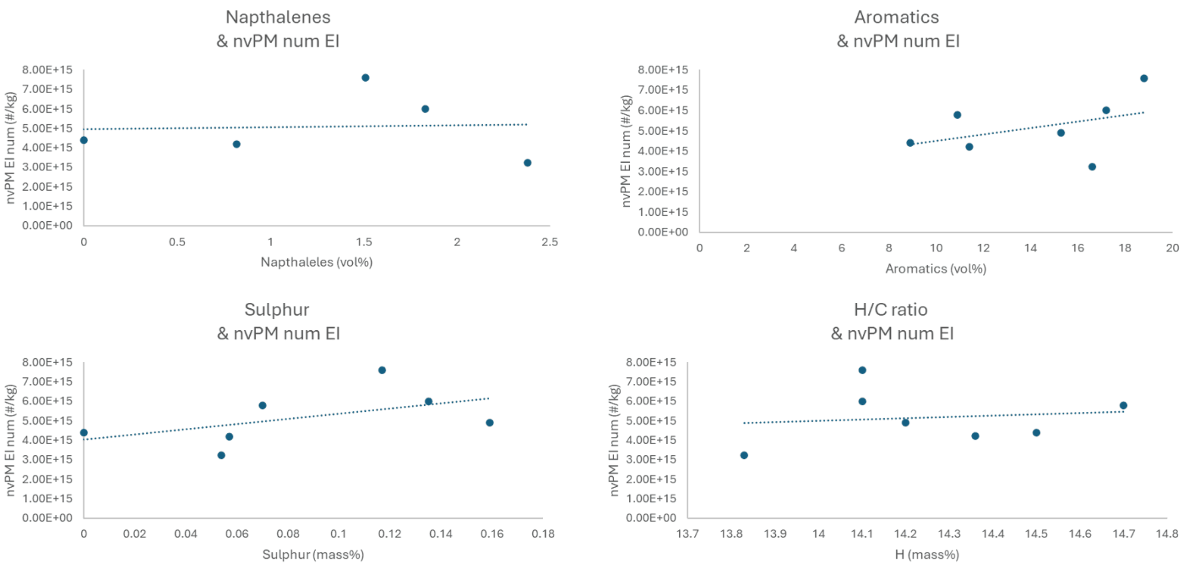

Figure 2.11 - nvPM number at mid power condition (42kN) vs fuel composition

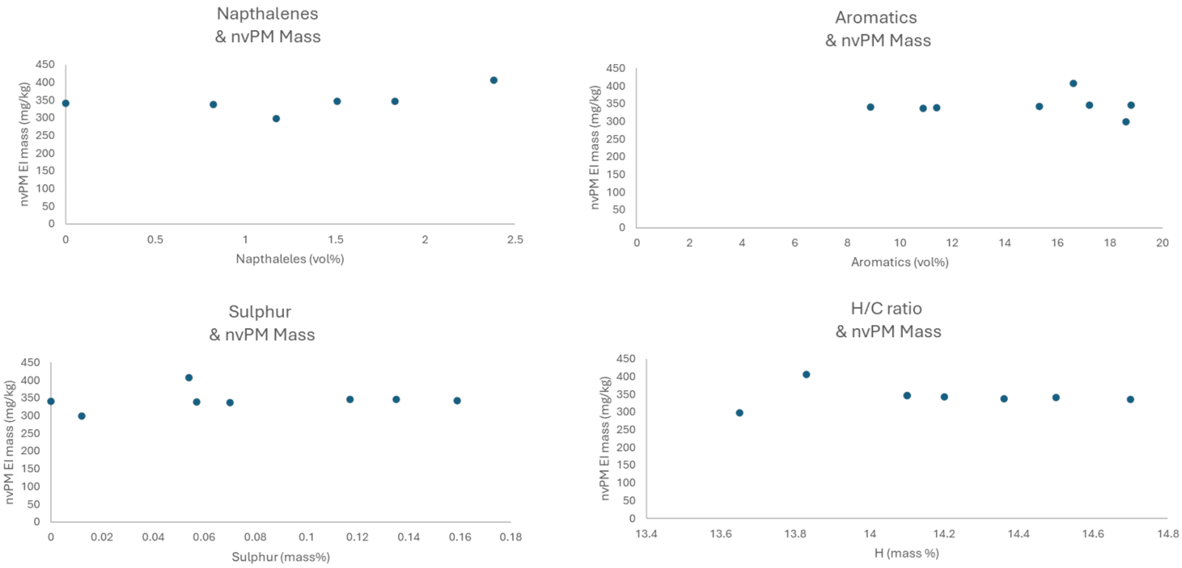

Figure 2.12 - nvPM number at high power condition (96kN) vs fuel composition

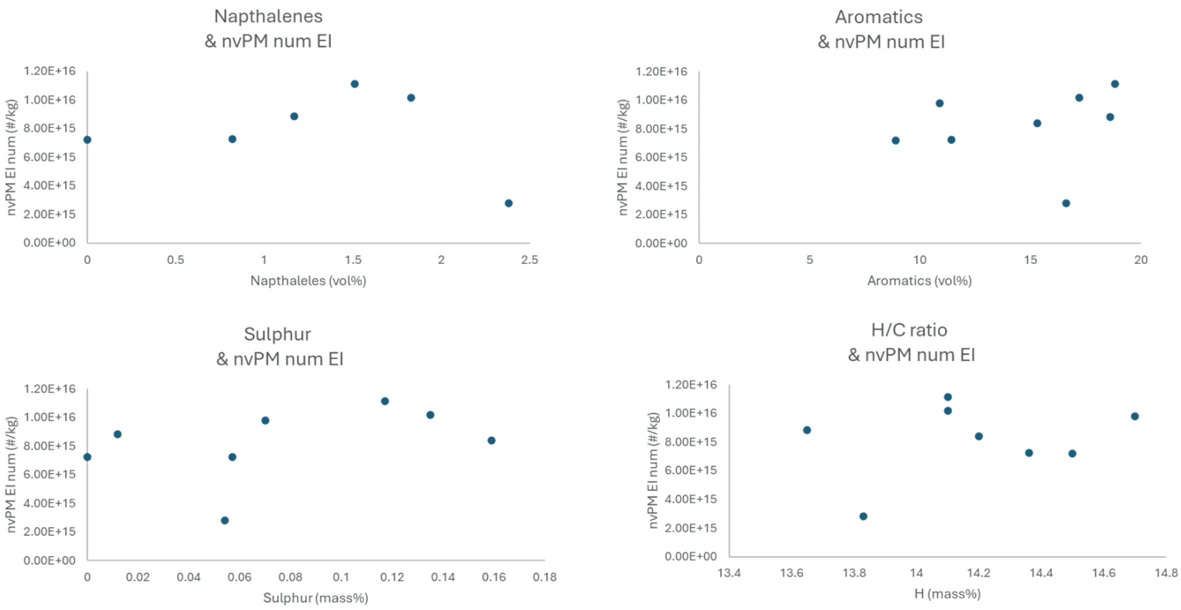

Figure 2.13 - nvPM number at high power condition (96kN) vs fuel composition

At the mid power condition, nvPM Mass EI scales in an approximately linear manner with Naphthalene volume content, aromatic volume content and hydrogen content. However, the nvPM Mass EI shows high degrees of scatter with sulphur content. Conversely, nvPM number scales with sulphur content and aromatic content, with a high degree of scatter. nvPM number at mid power appears to show little dependence on naphthalene content and hydrogen content.

At the high power condition, nvPM Mass EI scales in an approximately linear manner with Naphthalene volume content and hydrogen content. nvPM mass EI shows high degrees of scatter with sulphur content and aromatic content. nvPM number at high power appears to show little dependence on fuel composition in comparison with mid power results.

2.3. Aviation emissions calculation

The combustion products of the aircraft gas turbine engine are mainly composed of the carbon dioxide, water vapor, unburned hydrocarbons, carbon monoxide, nitrogen oxides, sulphur oxides, excess atmospheric oxygen and nitrogen, and soot [16-17]. In order to calculate total exhaust emissions during a flight segment, the emission index (EI), defined as the mass of pollutant emitted per unit mass of fuel burned for a specified engine, must be calculated for these emissions. CO_2, H_2O and SO_X emissions are directly proportional to fuel burned. However, HC, CO, NO_X and soot are affected by several parameters such as engine type, power setting, flight altitude and ambient atmospheric conditions. In the ICAO aircraft engine emission data bank (EEDB) [8], emissions of CO, HC, NO_X, non-volatile particulate matter (nvPM) and smoke number (SN), together with associated fuel flow rates, are provided at a set of four reference power settings defined as “take-off”, “climb”, “approach” and “idle”. ICAO EEDB is publicly available, and updates to the EEDB are made as new engines are certified. With the publication of Revision 28 in December 2020, the ICAO EEDB includes two primary datasets in separate spreadsheets. One spreadsheet holds the data for gaseous and smoke emissions, while the other contains data on nvPM emissions. Emissions indices provided in the ICAO EEDB can be directly used to calculate the amount of emissions of CO, HC, NO_X, nvPM mass and nvPM number below 3000 ft above ground level (AGL).

However, ICAO EEDB cannot be directly used to calculate the amount of emissions of CO, HC, NO_X, nvPM mass and nvPM number above 3000 ft AGL. The Boeing Fuel Flow Method 2 (BFFM2) [18], which is one of the most widely used methodologies to calculate in-flight emissions of HC, CO, and NO_X, is used to calculate the emissions above 3000 ft AGL. Additionally, the mission emissions estimation methodology (MEEM) [19], which is used to estimate in-flight nvPM emissions, is also employed for this purpose. Both BFFM2 and MEEM are developed with respect to conventional fuels and required modifications/extra steps have been detailed in the following sections to calculate the in-flight emissions of sustainable aviation fuels (SAFs).

2.3.1. Calculation of EIs for HC, CO and NO_X

BFFM2 is used to calculate the emissions indices of HC, CO, and NO_X at any flight altitude. Since BFFM2 relies on the engine's fuel flow parameter, which can be obtained through simulation or Flight Data Recorder (FDR) data, along with publicly available emission index values from the ICAO EEDB, it allows for the calculation of the emission indices for HC, CO, and NO_X at any flight altitude without requiring proprietary engine data [18].

The BFFM2 mainly consist of three main steps (numbered in black in Figure 2.10). The processes begins with the correction of the in-flight fuel flow rate to the corresponding sea level fuel flow rate (Equation 1). The corrected fuel flow is then used to obtain the corresponding emissions indices of HC, CO, and NOx at sea level which are used in the final step to calculate emissions indices at flight altitude. In the ICAO EEDB, fuel flow rates and emissions indices under the International Standard Atmosphere (ISA) conditions at sea level are given for different engine models for the following flight phases: take-off, climb, approach, and idle. A correlation between fuel flow rates and emissions indices at sea level is established using these four data points in order to calculate the corresponding emission index values for any fuel flow rate. Equations 2-4 are used in the last step of the BFFM2 process to correct the obtained sea level emissions indices at flight altitude.

$$ff_{sl} = ff_{alt}\frac{\theta_{amb}^{3.8}}{\delta_{amb}}exp^{0.2M^2} \qquad (1)$$

$$EIHC_{alt} = EIHC_{sl}\frac{\theta_{amb}^{3.3}}{\delta_{amb}^{1.02}} \qquad (2)$$

$$EICO_{alt} = EICO_{sl}\frac{\theta_{amb}^{3.3}}{\delta_{amb}^{1.02}} \qquad (3)$$

$$EINO_{X_{alt}} = EINO_{X_{sl}}\sqrt{\frac{\delta_{amb}^{1.02}}{\theta_{amb}^{3.3}}}e^{H} \qquad (4)$$

where $\theta_{amb} = \frac{T_{amb}[K]}{288.5}$, $\delta_{amb} = \frac{P_{amb}[Pa]}{101325}$ · ff_{sl} is the corrected fuel flow at sea level in (kg/s), ff_{alt} is the fuel flow at flight altitude (kg/s); $EIHC_{sl}$, $EICO_{sl}$ and $EINO_{x,sl}$ are HC, CO, and NO_X emissions indices at sea level respectively; $EIHC_{alt}$, $EICO_{alt}$ and $EINO_{x,alt}$ are HC, CO, and NO_X emissions indices at flight altitude respectively.

Finally, the total emission for a flight segment is calculated using Equation 5.

$$Total\ Emission(X) = E_n \cdot EI(X) \cdot TIM \cdot ff_{alt} \qquad (5)$$

where E_n, EI(X), and TIM denote the number of engines, emission index for pollutant X (g/kg fuel), and time in seconds respectively.

2.3.1.1. Calculation of EIs of HC, CO and NOx for SAF

The original BFFM2 was developed with respect to conventional fuels and does not take into account the type of fuel used. Therefore, some modifications are needed to calculate altitude emissions while utilising SAF considering as well their blends. Analysing the BFFM2 application process shown in Figure 2.14, it reveals that Step 1 and Step 2 (numbered in black color) require modifications. Step 3, which corrects the sea level emission index to the flight altitude and independent from the type of fuel used, does not require modification.

Fusaro et al. [20] modified the original BFFM2 to extend it to supersonic speed regime and different types of fuels. They called the updated method as Sustainable Supersonic Fuel Flow Method (S2F2). The engine fuel flow rate correction, according to the original BFFM2 paper, is derived from the energy balance across the combustor. According to Fusaro et al. [20] the lower heating value (LHV), an energetic index that represents the fuel energy content, or the amount of energy the fuel can release, is the most significant of all the factors of the energy balance through the combustor. Therefore, the LHV of conventional fuel and SAF blend can be used to adjust the in-flight fuel flow of pure conventional fuel, allowing for the calculation of the corresponding fuel flow value for the SAF blend. Therefore, LHV property of conventional and SAF blend can be used to correct the in-flight fuel flow of pure conventional fuel in order to obtain corresponding fuel flow value of SAF blend. Insight of this knowledge, the fuel flow rate correction developed with respect to conventional fuel can be updated with a coefficient (K_{blend}) derived from the LHV of conventional fuel and LHV of the blend of different fuels.

$$K_{blend} = \frac{LHV_{conv}}{LHV_{blend\ \%z}}, \qquad (6)$$

where z is the percentage of SAF in the SAF blend, LHV_{conv} is the LHV of pure conventional fuel and $LHV_{blend\ z\%}$ is the LHV of the SAF blend. According to Zschocke et al. [21] and Striebich et al. [22], the LHV of a fuel blend is linear with respect to the blend ratios of fuels. Therefore, $LHV_{blend\ z\%}$ is calculated as [20];

$$LHV_{blend\ z\%} = \frac{LHV_{100\ \%SAF} \cdot z + LHV_{conv}(100-z)}{100}, \qquad (7)$$

where $LHV_{100\%SAF}$ is the LHV of the pure SAF. Consequently, corrected fuel flow rate in original BFFM2 was modified for SAF blend as;

$$ff_{sl} = ff_{alt} K_{blend} \frac{\theta_{amb}^{3.8}}{\delta_{amb}} e^{0.2M^2}. \quad (8)$$

On the other hand, the remaining equations of BFFM2 are left as the original ones since the authors still use the EIs of conventional fuel from the ICAO EEDB.

We aim to improve the modified BFFM2 developed by Fusaro et al. [20] to estimate the emissions of SAF at different blending ratios. For that, we consider two approaches: (i) to apply a more accurate fuel flow correction factor to conventional fuel, (ii) to modify the sea level EI model of the conventional fuel by applying a SAF-correction factor to emission indices of the ICAO databank. The resulting improved model will reduce the error in emissions estimation during flight using SAFs considering as well the blends.

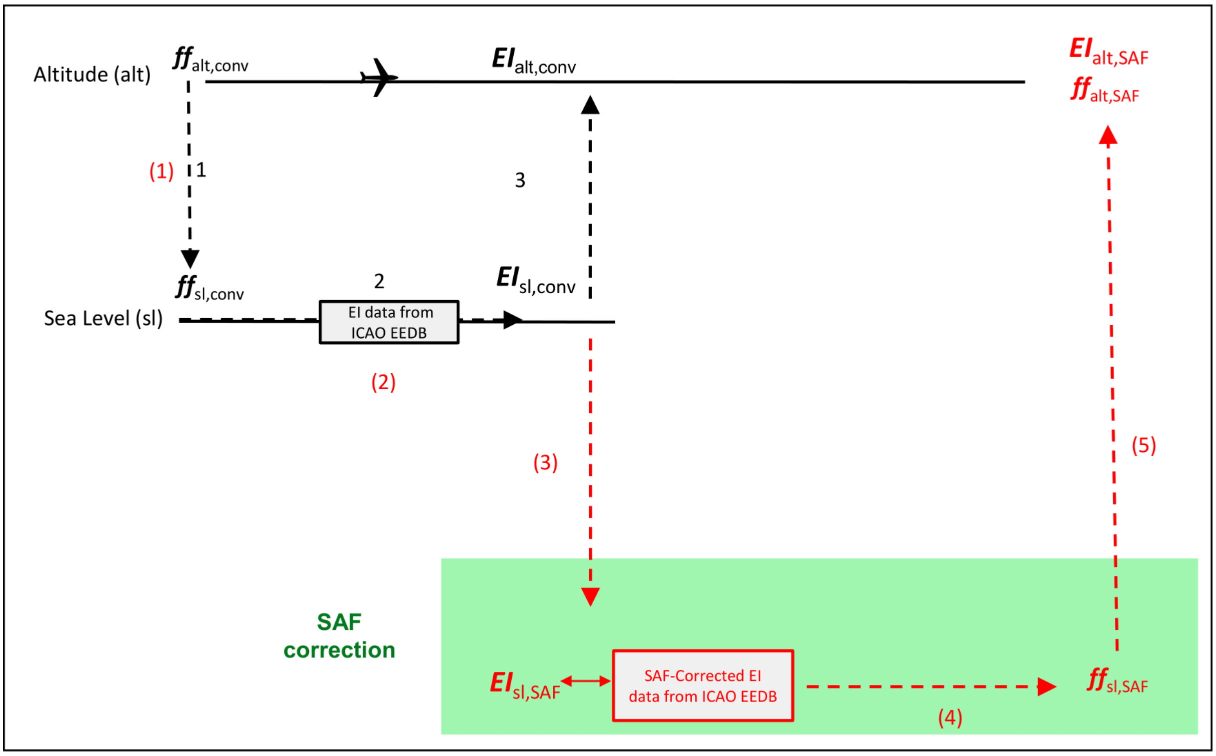

Figure 2.14 - Process of the proposed SAF-modified BFFM2

Each step of the proposed modified BFFM2, which aims to improve the S2F2 methodology developed by Fusaro et al. [20], are given in Figure 2.14. The three main steps of the original BFFM2 are numbered in black color in Figure 2.14. The proposed modified BFFM2 consists of 5 steps (numbered in red color) and, both fuel flow correction and EI correction are carried out at sea level conditions. The first step is the same as the original BFFM2 and correlates the in-flight fuel flow of conventional fuel to sea level conditions. The second step is to find the emission indices of HC, CO and NOx corresponding to fuel flow rate of conventional fuel calculated in Step 1. In the third step, correction factors are applied to the emission indices of conventional fuel to derive the corresponding emission indices for SAF blend. The details of how we plan to correct the emission indices for SAF blends are provided in the following section. In the fourth step, the correction factor, K_{blend}, is applied to the fuel flow of conventional fuel at sea level to determine the corresponding fuel flow of SAF blend at sea level. The details for calculating K_{blend} are provided in the following paragraph. The last step is to apply pressure correction to sea level emission indices of SAF blend and to apply fuel flow rate correction (inverse of step 1) to sea level fuel flow of SAF blend to calculate corresponding in-flight emission indices and fuel flow values of SAF blend.

Our goal is to more accurately estimate the fuel flow value for SAF blends, $ff_{sl,SAF}$ under sea level conditions when using these blends instead of pure conventional fuels. When analysing the energy balance equation provided in the original BFFM2, burner efficiency emerges as another important factor within the energy balance across the combustor. As a part of thermodynamic efficiency, combustion efficiency can be used with the LHV property since several studies examining the fuel and emission performance of SAFs have reported significant differences in combustion efficiency for low power settings compared to conventional fuels [23], [24]. Given this information, we decided to redefine the K_{blend} - fuel flow correction factor. Unlike the previous definition established solely as a function of LHV by Fusaro et al. [20], our redefinition incorporates both LHV and combustion efficiency to enhance its accuracy. We use Equation 9 which computes the combustion efficiency (η) based on the emissions indices of HC and CO [16].

$$1 - \eta_c = \left(EI_{HC} + 0.232 EI_{CO}\right)10^{-3} \tag{9}$$

The new K_{blend}- fuel flow correction factor is defined as:

$$K_{blend} = k_1 k_2, \tag{10}$$

where

$$k_1 = \frac{LHV_{conv}}{LHV_{blend\ z\%}}, \qquad k_2 = \frac{\eta_{c,conv}}{\eta_{c,blend\ z\%}}, \tag{11}$$

$\eta_{c,conv}$ and $\eta_{c,blend\ z\%}$ represent the combustion efficiencies of conventional fuel and the SAF blend, respectively. Engine emissions indices provided in ICAO EEDB for conventional type fuel can be used as a reference and we can update these EIs for

SAF blends at sea level. In order to update the EIs of conventional fuel, we aim to calculate emission index correction factors, $E_{blend,HC}$, $E_{blend,CO}$ and $E_{blend,NOx}$ as we did for fuel flow correction. We define two approaches to calculate emission index correction factors for the modification of the EIs provided in ICAO EEDB for conventional fuel: (i) use literature data to apply a correction factor to EIs of conventional fuels (ii) perform chemical kinetic modelling of the engine combustion process to estimate EIs of conventional fuel-SAF blends. At this point, we could not reach enough data from literature to obtain a correction factor but, the research team from University of Birmingham is about to finish the chemical kinetic modelling of the engine combustion process to estimate EIs of conventional fuel-SAF blends. After obtaining the correction factors to be applied to the EIs of the conventional fuel, EIs of SAF blend at sea level can be calculated as:

$$EIHC_{sl,blend} = EIHC_{sl,conv} E_{blend,HC} \tag{12}$$

$$EICO_{sl,blend} = EICO_{sl,conv} E_{blend,CO} \tag{13}$$

$$EINOx_{sl,blend} = EINOx_{sl,conv} E_{blend,NOx} \tag{14}$$

2.3.2. Calculation of EI for Non-Volatile Particulate Matter (nvPM)

The MEEM developed by Ahrens et al. [19] is one of the methodologies used to calculate the non-LTO emissions of nvPM mass (EI_{mass}) and nvPM number (EI_{number}) at altitude. The method is considered as the synthesis and improved version of the previously developed methods and is used in a similar manner as BFFM2. The method relies on the LTO nvPM emissions data from the ICAO EEDB, but also allows for previously certified engines which do not have data in the EEDB. For these previously certified engines that do not have nvPM LTO data in EEDB, the nvPM emissions indices are estimated from their smoke number certification values using the SCOPE11 correlative methodology developed by [25].

The flowchart of the MEEM method is presented in Figure 2.11. This method was developed for conventional fuels, and when applied to calculate EI_{mass} and EI_{num} for these fuels, it involves four main steps, numbered in black in Figure 2.15. Additionally, for engines that do not have nvPM data available in the EEDB, an extra preliminary step (Step 0) is included in the MEEM method. This step allows us to calculate the EI_{mass} and EI_{num} from smoke number data for the four LTO conditions. This step is essentially the First Order Approximation v4.0 (FOA4.0) method for estimating EI_{mass} and EI_{num}. FOA4.0 is based on the SCOPE11 method [25], with each step of FOA4.0 detailed in a separate subsection.

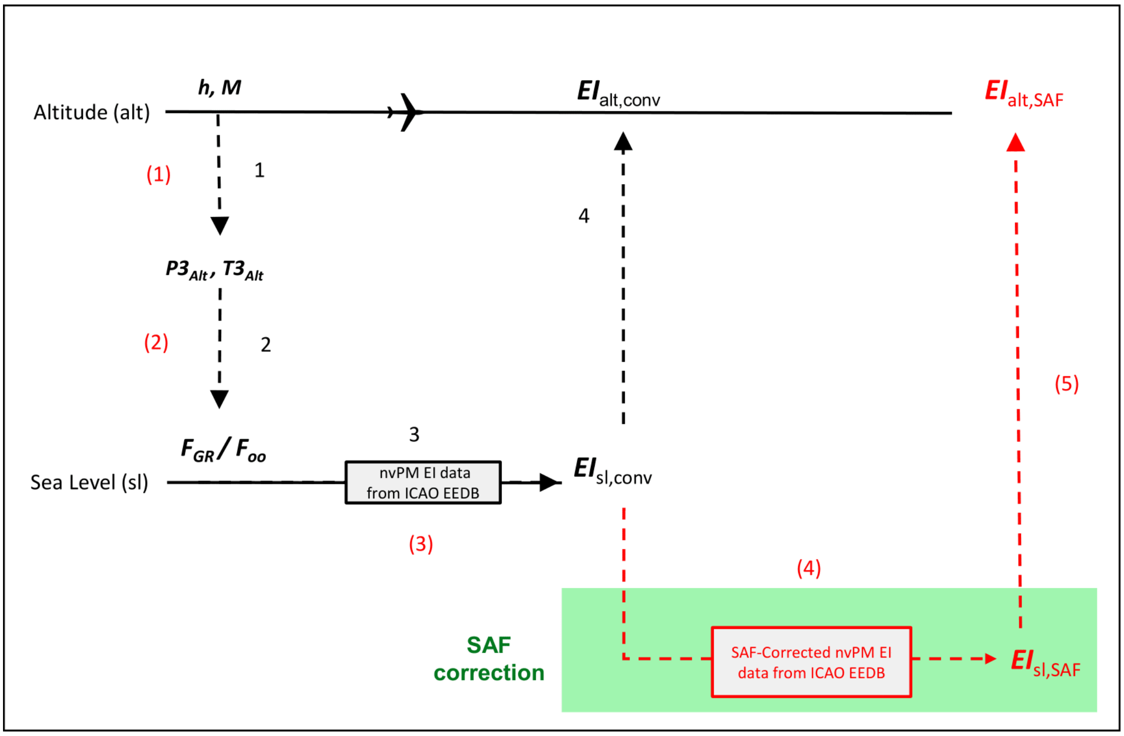

Figure 2.15 - The flow chart of MEEM method for conventional fuels (numbered in black) and SAF blends (numbered in red)

Step 1 of the MEEM method is to estimate the temperature and pressure at the combustion chamber inlet ($T3_{Alt}$ and $P3_{Alt}$) for the corresponding flight condition, using altitude and Mach number as inputs. In Step 2, the ground reference state (GR) is established by assuming that the combustor inlet temperature at ground conditions ($T3_{GR}$) is equal to $T3_{Alt}$. Under this assumption, an engine producing the thrust, F_{GR}, would have the same T3 as under altitude conditions. Based on this, the necessary calculations are performed to determine the ground reference combustor inlet pressure ($P3_{GR}$) and thrust (F_{GR}). Once F_{GR} is known, the ratio (F_{GR}/F_{00}) is calculated, where F_{00} represents the engine's nominal rated thrust. Step 3 uses interpolation to estimate nvPM mass and number emission indices corresponding to the F_{GR}/F_{00} ratio based on data from the ICAO EEDB. Finally, Step 4 computes in-flight nvPM mass and number emissions by applying a ground-to-flight transposition correlation. Each step of the MEEM method is described in detail in the original paper by [19].

2.3.2.1. First Order Approximation V4.0 Method (FOA4.0)

FOA 4.0 is a method for estimating engine exhaust particulate emissions. It is derived from the SCOPE11 method [25], and follows the procedures established therein. Consistent with the SCOPE11 method, FOA4.0 starts by calculating the nvPM concentration, denoted as CI_{mass}.

$$CI_{mass}\left[\frac{\mu^3}{kg}\right] = \frac{648.4e^{0.0766\,SN}}{1+e^{-1.099\,(SN-3.064)}}. \tag{15}$$

The emission index of nvPM mass is calculated by multiplying CI_{mass} by volumetric flow, Q_{mode} · Q_{mode} depends on the air fuel ratio (AFR) and reference by-pass ratio (β).

$$Q_{mode}\left[\frac{m^3}{kg}\right] = 0.776 \cdot AFR \cdot (1 + \beta) + 0.767 \tag{16}$$

The AFR at each of the four LTO points has been estimated by [26] as 106 at Idle, 83 at Approach, 51 at ClimbOut, and 45 at Take-Off. The value of β depends on the engine exhaust configuration. Engines with mixed nozzles ("MTF" in the EEDB) require a correction for the β, and therefore β is the by-pass ratio. For all other engines (e.g. "TF" in the EEDB), set β = 0.

The nvPM mass concentration at the measurement instrument is always lower than at the engine exit plane due to particle losses in the sampling system. Therefore, a correction factor, k_{slm}, is used to account for the measurement system loss. It depends on the reference by-pass ratio, β and the nvPM concentration, CI_{mass}.

$$k_{slm} = ln\left(\frac{3.219CI_{mass}(1+\beta)+312.5}{CI_{mass}(1+\beta)+42.6}\right). \tag{17}$$

Finally, the product of CI_{mass}, Q_{mode} and k_{slm} gives the nvPM EI_{mass} for the four LTO conditions.

$$EI_{mass}\left[\frac{mg}{kg}\right] = CI_{mass} \cdot Q_{mode} \cdot k_{slm} \tag{18}$$

The estimation of nvPM number, EI_{number}, requires EI_{mass} and engine mode-dependent geometric mean diameters (GMD) of the nvPM particles. GMD recommended values for LTO modes are: Idle:20 nm, Approach: 20 nm, Climb-Out: 40 nm, Take-Off: 40 nm. Based on these values, EI_{num} is calculated as:

$$EI_{num}\left[\frac{\#}{kg}\right] = \frac{EI_{mass}}{\frac{\pi}{6}10^9\left(\frac{GMD}{10^9}\right)e^{4.5(ln(1.8))^2}}. \tag{19}$$

2.3.2.2. Calculation of EI of nvPM for SAF

Emissions of nvPM for SAF can be calculated by the combination of MEEM and methodology proposed by Teoh et al. [27]. In MEEM, corresponding EI_{mass} and EI_{number} at sea level are estimated by using the ratio of calculated ground thrust (F_{GR}) and the nominally rated thrust of the engine (F_{00}), (F_{GR}/F_{00}). The fuel to be used instead of conventional fuel must be 'drop in'. In other words, pure SAF or SAF blends should be able to replace conventional fuel in a manner that does not require modification of the aircraft/engine fuel systems or result in different engine performance [20,28-29]. Therefore, if the changes in EI_{mass} and EI_{number} at sea level are estimated in the case of using SAF, we can still use the same ratio (F_{GR}/F_{00}) to estimate corresponding SAF nvPM emission indices.

The methodology proposed by Teoh et al. [27] can be used to estimate the reduction in EI_{number} and EI_{mass} when using SAF instead of conventional fuels. The proposed methodology is based on the difference in hydrogen mass content (ΔH) between the reference fuel and SAF, and the ratio of calculated ground thrust and the nominally rated thrust of the engine defined as $\hat{F} = \left(\frac{F_{GR}}{F_{00\infty}}\right)$. ΔEI_{number} and ΔEI_{mass} are estimated from the formula given as:

$$\Delta EI_{number}(\%) = \left(-\ 114.21\ +\ 1.06\hat{F}\right)\Delta H, \qquad when\ \Delta H \leq 0.5\%$$
$$\left(-\ 114.21\ +\ 1.06\hat{F}\right)\Delta H \cdot e^{(0.5-\Delta H)} \quad when\ \Delta H\ >\ 0.5\% \qquad (15)$$

where

$$\Delta H\ = H_{SAF} - H_{ref}$$

ΔEI_{mass} and ΔEI_{number} correspond to the percentage reduction in nvPM mass and nvPM number, $\hat{F}$ is the percentage of engine thrust in percentage, H_{SAF} is the hydrogen content of SAF fuel, H_{ref} is the hydrogen content of the reference (conventional) fuel, and ΔH is the change in hydrogen mass content.

In addition to utilizing Teoh's methodology, University of Birmingham developed new equations based on literature data to estimate reductions in PM emissions.

After calculating the expected reductions in nvPM mass and nvPM number when using SAF or SAF blends instead of conventional fuel, the nvPM mass and nvPM number for SAF or SAF blends can now be calculated.

$$EI_{mass,blend} = EI_{mass,conv} \cdot \frac{100-\Delta EI_{mass}}{100}, \qquad (22)$$

$$EI_{number,blend} = EI_{number,conv} \cdot \frac{100-\Delta EI_{number}}{100}. \qquad (23)$$

$EI_{mass,conv}$ and $EI_{number,conv}$ represent the nvPM mass and number emissions for conventional fuel, while $EI_{mass,blend}$ and $EI_{number,blend}$ represent the nvPM mass and number emissions for SAF blends.

2.3.3. Calculation of Fuel Properties and fuel composition-based EIs

The prediction of emissions for SAF fuel blends from the EEDB requires knowledge of the hydrogen content, calorific value and Sulphur content of the conventional fossil derived fuel and the SAF product which are blended together. For newer engine cases in the EEDB, where nvPM emissions tests are carried out at the same time as gaseous emissions, sufficient information is available to determine these fuel properties from the EEDB worksheet named "nvPM Emissions". However, if the nvPM measurements are not made at the same time as the reported gaseous emissions data in the EEDB, then it is not possible to extract these values from the EEDB as they are not reported in the same way for the ICAO engine certification for gaseous emissions. In such cases, an alternative route to estimate the missing fuel properties is proposed, using average values for these key properties taken from available fuel property surveys to allow the analysis to proceed (Figure 2.12).

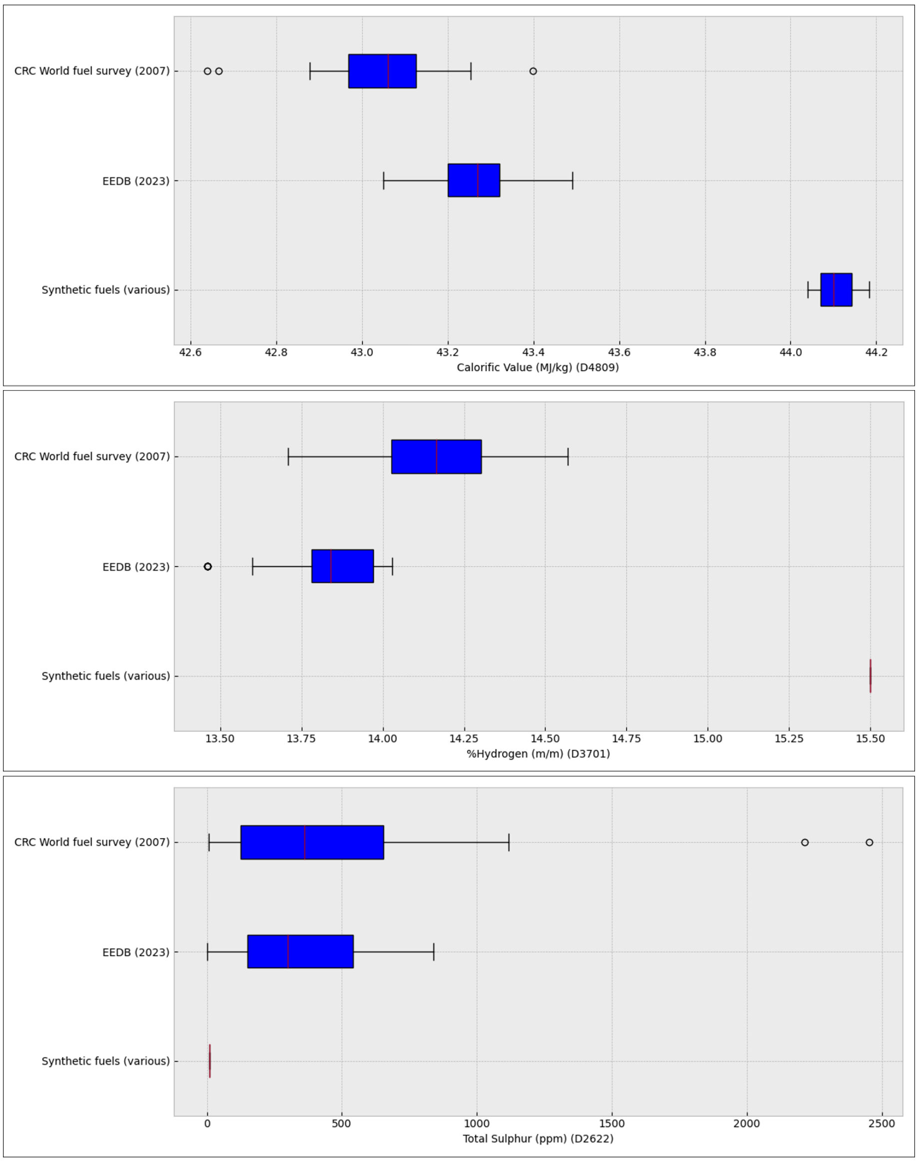

Figure 2.15 - Average properties chart for conventional fuels and synthetic fuels [3].

2.3.3.1. Calculation of Lower Heating Value of SAF Blends

Several studies in the literature reported that the LHV of a fuel blend is linear with respect to the blend ratios of neat fuels [21-22,30-31]. Therefore, the lower heating value of the blend, denoted as LHV_{blend}, is calculated as the sum over all i-th components of the product of the weight fraction (w_i) of the neat blend component and the lower heating value (LHV_i) of that component:

$$LHV_{blend} = \sum_i w_i \cdot LHV_i \qquad (24)$$

where LHV_{blend} is the lower heating value of the blend, w_i is the weight fraction of the i-th neat blend component, and LHV_i is the lower heating value of the i-th neat blend component.

2.3.3.2. Calculation of Hydrogen Content of SAF Blends

Several studies in the literature reported that the H content of a fuel blend is linear with respect to the blend ratios of neat fuels [22,30-31]. Therefore, the hydrogen content of the blend, denoted as H_{blend}, is calculated as the sum over all components i of the product of the weight fraction (w_i) of the neat blend component and the hydrogen content (H_i) of that component:

$$H_{blend} = \sum_i w_i \cdot H_i, \qquad (25)$$

where H_{blend} is the hydrogen content of the blend, w_i is the weight fraction of the neat blend component i, and H_i is the hydrogen content of the i-th neat blend component.

2.3.3.3. Calculation of EI for H_2O

The assumption that all the hydrogen in the fuel has been converted to H_2O does not take into account the combustion efficiency of the combustor and fuel combination at the flight conditions concerned. Under real combustion conditions, there is always an emission of HCs. By incorporating a correction factor based on the hydrogen content of the blended fuel and the fuel used in the ICAO emissions database and a factor based on combustion efficiency, as defined in Equation (9), a more accurate estimation of water vapour emission could be made as:

$$EI_{H_2O,blend}\left(\frac{g}{kg}\right) = EI_{H_2O,conv}\frac{H_{blend}}{H_{conv}}\frac{\eta_{c,blend}}{\eta_{c,conv}}, \qquad (26)$$

where $EI_{H2O,conv}$, H_{conv}, and η_{conv} represents the H_2O, hydrogen content and combustion efficiency for conventional fuel, while $EI_{H2O,blend}$, H_{blend}, and η_{blend} represents the H_2O, hydrogen content and combustion efficiency for SAF blend.

2.3.3.4. Calculation of EI for CO_2

The assumption that all the carbon in the fuel has been converted to CO_2 does not take into account the combustion efficiency of the combustor and fuel combination at the flight conditions concerned. Under real combustion conditions, there is always an emission of CO and HCs. By incorporating a correction factor based on the carbon content of the blended fuel and the fuel used in the ICAO emissions database and a factor based on combustion efficiency, as defined in Equation (9), a more accurate estimation of carbon dioxide emission could be made as:

$$EI_{CO_2,blend}\left(\frac{g}{kg}\right) = EI_{CO_2,conv}\frac{C_{blend}}{C_{conv}}\frac{\eta_{c,blend}}{\eta_{c,conv}}, \quad (27)$$

or

$$EI_{CO_2,blend}\left(\frac{g}{kg}\right) = EI_{CO_2,conv}\frac{100-H_{blend}}{100-H_{conv}}\frac{\eta_{c,blend}}{\eta_{c,conv}}, \quad (28)$$

where $EI_{CO2,conv}$ and C_{conv} represent the CO_2 and carbon content for conventional fuel, respectively, while $EI_{CO2,blend}$ and C_{blend} represent the CO_2 and carbon content for SAF blend, respectively. To determine the carbon content of conventional fuel, we can apply the principle of conservation of mass and utilize the known mass fraction of hydrogen present in the fuel. Assuming kerosene comprises only carbon and hydrogen, we calculate the carbon weight percentage by subtracting the hydrogen weight percentage hydrogen from 100%. This method ensures the total equals 100%.

2.3.3.5. Calculation of EI for Sulphur Dioxide(SO_2) and Sulfate (SO_4^{2-})

Sulphur contained in the fuels burned by aircraft engines emerges as the source of both SO_2 and Sulphate emissions. Fuel sulphur is first oxidized in the combustor of jet engines, and it is released at the engine's exit plane primarily as SO_2. Sulphate is formed from the fuel sulphur via oxidation of SO_2 to SO_3 and subsequent hydration, in the exhaust plume, of SO_3 to H_2SO_4 .The fuel sulphur content is the only factor that affects both emissions; flight altitude and engine power settings have no effect [17,32-33].

The EIs of SO_2 and Sulfate are calculated from the formula given in [17, 32] as:

$$EI_{SO_2}\left(\frac{mg}{kg}\right) = 10^6\left[\frac{FSC\cdot(1-\varepsilon)\cdot MW_{SO_2}}{MW_{Sulphur}}\right]\cdot S_r, \quad (29)$$

$$EI_{sulphate}\left(\frac{mg}{kg}\right) = 10^6\left[\frac{FSC\cdot\varepsilon\cdot MW_{SO_4^{2-}}}{MW_{Sulphur}}\right]\cdot S_r, \quad (30)$$

where MW_{SO2} is the molecular weight of the SO_2 equal to 64, $MW_{sulfate}$ is the molecular weight of the SO_4^{2-} equal to 96, $MW_{Sulphur}$ is the molecular weight of elemental sulphur equal to 32, FSC is fuel sulphur content (mass fraction), ε is fuel sulphur conversion efficiency (mass fraction, e.g 0.02), and S_r is the unit scale factor equal to 1 mg/kg.

Since the EIs of SO_2 and sulphate only depend on the sulphur content of the fuel, Equation 29 and 30 can be used for both conventional fuels and SAF blends. The sulphur content of each neat fuel component can be used in the same way as the computation of hydrogen and LHV of blends to get the sulphur content of the SAF blend.

$$FSC_{blend} = \sum_i w_i \cdot FSC_i , \qquad (31)$$

where FSC_{blend} is the sulphur content of the blend, w_i is the weight fraction of the i-th neat blend component, and FSC_i is the sulphur content of the i-th neat blend component. Now, it is possible to calculate EIs for SO_2 and sulphate for SAF blends by replacing the FSC in Equation (29) and (30) with FSC_{blend}.

3. Air quality modelling

3.1. Atmospheric chemistry transport modelling (TUD)

3.1.1. Introduction

Aircraft emissions are responsible for releasing chemical products in the atmosphere, such as NO_2, CO_2, PM of different sizes, BC, etc. These products are reported to have climate and air quality effects, such as contributing to the greenhouse effect and degradation of local air quality, which are associated with health diseases and premature deaths.

Aircraft emissions take place during flight (cruise emissions) as well as during taxiing, manoeuvring, and landing and take-off operations (LTO). The latter are of particular interest since they take place near airports and urban areas, and the release of certain pollutants, e.g., $PM_{2.5}$, may lead to alterations of the local atmospheric composition, e.g., ozone formation/depletion, which may directly affect local air quality.

The investigation of the effects of aircraft emissions in the vicinity of airports, how they impact local air quality, and potential ways of mitigating their negative impacts, including those from the introduction of sustainable aviation fuels, is a topic of public interest due the fact that they are directly related to impacts on human health.

3.1.2. Objectives

The objective of the research at TU Delft is to investigate the impacts of aircraft emissions during LTOs near airports. In order to be able to progress in parallel with the other activities, aircraft emissions during LTOs are initially taken from the Open Aviation Emissions Model (openAVEM) and the data is integrated into the high performance version of the atmospheric chemistry model solver GEOS-Chem (GCHP).

3.1.3. Methods

3.1.3.1. openAVEM

In order to calculate aviation emissions related to LTO, the present work makes use of the Open Aviation Emissions Model (openAVEM) software [34], [35] which is a Python based package that evaluates fuel burn and atmospheric emissions based on a list of flights as input data. openAVEM is able to provide data from LTO only and full-flight aviation emissions separately.

Monthly emissions are then incorporated into a 3D grid with a 0.5° latitude by 0.625° longitude by 500 ft altitude resolution, which serves as input for the atmospheric chemistry transport model solver GEOS-Chem. The monthly data provided by openAVEM allows for an evaluation of LTO related emissions, as well as their impacts on local air quality.

Flight emissions are calculated based on data from OAG , Flightradar24, and OpenSky. Emissions indices of NO_X, CO, HC, and nvPM are taken mainly from the ICAO Engine Emissions Databank. Additional data for piston engines are based on data from the Swiss Federal Office of Civil Aviation, and on the data from the US Environmental Protection Agency or from Stettler [36] for older engine models. The emissions due to Auxiliary Power Units (APU) are modelled with times-in mode and the emissions indices are modelled according to aircraft type, in accordance with the ICAO's Airport Air Quality Manual [35].

The emissions of NO_X, CO, HC follow from the Boeing Fuel Flow Method 2, with NO_X expressed as NO_2 equivalent, and HC as CH_4 equivalent. As for non-volatile particulate matter, the emissions indices are taken from the ICAO database (if available). Otherwise, the emissions indices are estimated from smoke numbers using the FOA 4.0 method. If the smoke number is not available, a constant value of 0 and 30 mg/kg are employed for LTO and non-LTO, respectively [35].

3.1.3.2. GEOS-Chem High Performance

One possibility to evaluate aircraft emissions and how they impact local air quality is to make use of atmospheric chemistry transport model codes. One such code is the high-performance version of GEOS-Chem (GCHP) [37], which solves the continuity equation for multiple chemically active species, according to [37]

$$\frac{\partial n_i}{\partial t} + \nabla \cdot (n_i u) = s_i ,$$

where n_i is the species number density in $molec \cdot cm^{-3}$, $\mathbf{u}$ is the wind speed in $m \cdot s^{-1}$, and s_i is the production rate of species i in $molec \cdot cm^{-3} \cdot s^{-1}$.

GCHP makes use of cubed-sphere (CS) grids which can be of two types: standard or stretched CS grids. The latter is a CS grid which has regions with different horizontal resolution as opposed to the standard CS in which the grid is uniform with equal sized elements throughout the domain.

GCHP makes use of the so-called cubed-sphere grids which consist of a grid with six faces, and each face being divided into N by N elements. The so-called C24 grid, for instance, has 24 by 24 elements in each of the six grid faces.

Stretched-cubed-sphere grids are obtained by performing a Schmidt transform in a regular cubed-sphere grid [38]. This alters the cubed-sphere grid by increasing the element density in a region of interest and by decreasing the grid density outside of said region. Note that this procedure increases the grid density in a region, whereas decreasing in others, but it does not increase the number of grid elements.

In order to obtain a stretched-grid which features a refinement in an area of interest, it is necessary to define three parameters: the stretch factor (s), a target latitude, and a target longitude. The results presented in this deliverable are based on a stretched C24 grid, with stretch factor $s = 9.7$, target latitude 50.6^o North, target longitude 8.6^o East, see figure 3.1.

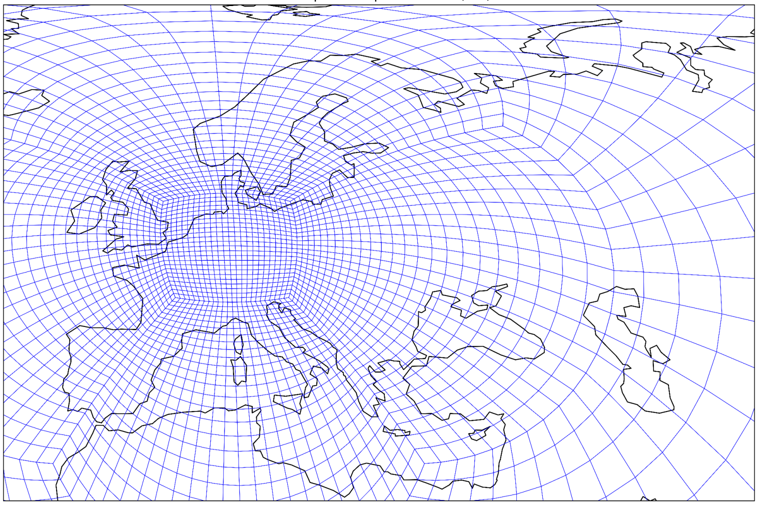

Figure 3.1 - Stretched cubed-sphere grid based on a C24 grid resolution used for the simulations.

3.1.3.3. Simulations

Firstly a one year spin-off simulation for the year of 2018 is performed in order to remove artefacts and to stabilise the simulation. The results of the spin-off year are then used as input data for simulating the year of interest. In the present case the spin-off year is 2018 and the year of interest to be analysed is 2019.

In order to obtain the LTO attributable air quality impacts, two simulations are required: one in with LTO emissions as well as emissions from other sources (here termed as background emissions), and a second one which does not include any emissions from aviation sources and simulates only background emissions. Then the results of the two simulations are subtracted from each other so that the LTO attributable effects can be investigated. The concentration maps of three species, ozone, nitric oxide, and $PM_{2.5}$, will be analysed to identify the effect aviation emissions have near airports.

3.1.4. LTO attributable air quality effects

The analysis of the local air quality impacts of aviation in the vicinity of airports is based on the annual-averaged concentration of three species of interest, namely $PM_{2.5}$, black carbon, and ozone at ground level. For the present case, the year of choice was 2019 and the aviation emissions accounted for were those related to LTO only.

It can be seen from Figure 3.2, that there is an increase in black carbon ground levels near the main European airports of up to $\sim 5\times10^{-3}\ \mu gC\cdot m^{-3}$. The annual-averaged concentration map of $PM_{2.5}$ is more dispersed than that of black carbon, but on comparing both maps, it can be seen that the area of $PM_{2.5}$ increase coincides with that of black carbon. For $PM_{2.5}$ an increase of up to $\sim 0.3\ \mu g\cdot m^{-3}$ due to LTO emissions.

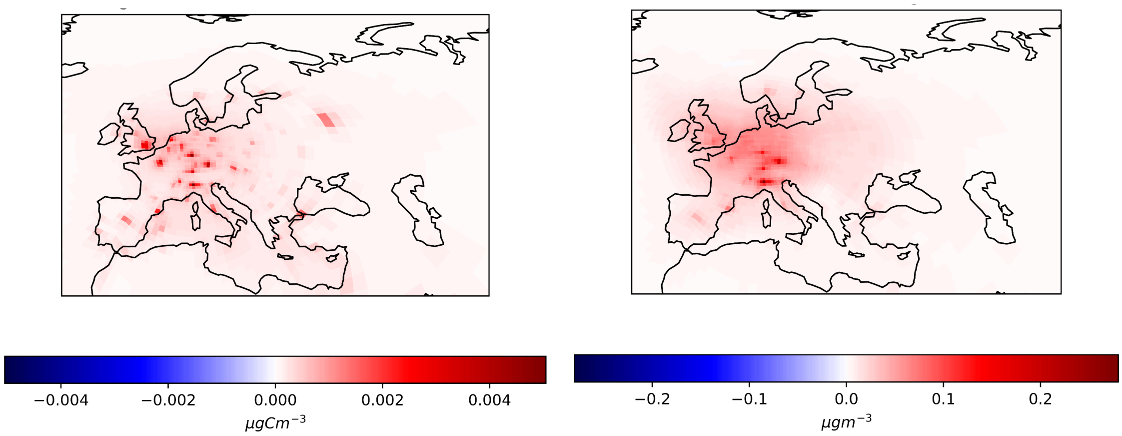

Figure 3.2 - LTO attributable annual-averaged mass of black carbon aerosol in $\mu gC\cdot m^{-3}$ (left) and $PM_{2.5}$ in $\mu g\cdot cm^{-3}$ (right) in Europe at ground level.

Nitrogen oxides NO_X (nitrogen dioxide, NO_2, and nitric oxide, NO) emitted from aircrafts interact with the atmospheric ozone, leading to ozone depletion. This interaction depends on both the layer of the atmosphere the emissions take place in, and time of the day. For tropospheric emissions, and during daytime, the photolysis of NO_2 lead to the formation of NO and the radical O. This radical can react with oxygen, which will lead to the formation of ozone. A third reaction may take place, in which ozone interacts with NO, which will result in the depletion of ozone [39].

$$NO_2 \rightarrow NO + O, \qquad (32.a)$$

$$O_2 + O \rightarrow O_3, \qquad (32.b)$$

$$NO + O_3 \rightarrow NO_2 + O_2, \qquad (32.c)$$

During nighttime, in the absence of sunlight, photolysis does not take place, so most of the NO_X is in the form of NO_2, which reacts with atmospheric ozone according to the following reaction [39].

$$NO_2 + O_3 \rightarrow NO_3 + O_2. \qquad (33)$$

Figure 3.3 shows the annual-averaged concentration map of ozone at surface level, where it can be seen that there is a reduction in ozone levels in areas near airports of up to $\sim 0.3\, ppbv$, whereas the LTO attributable surface levels of NO_2 and NO increase in the same locations. From the results, it becomes clear that aircraft emissions associated with LTO lead to peaks of nitrogen oxides, which in turn, lead to ozone depletion around the same areas.

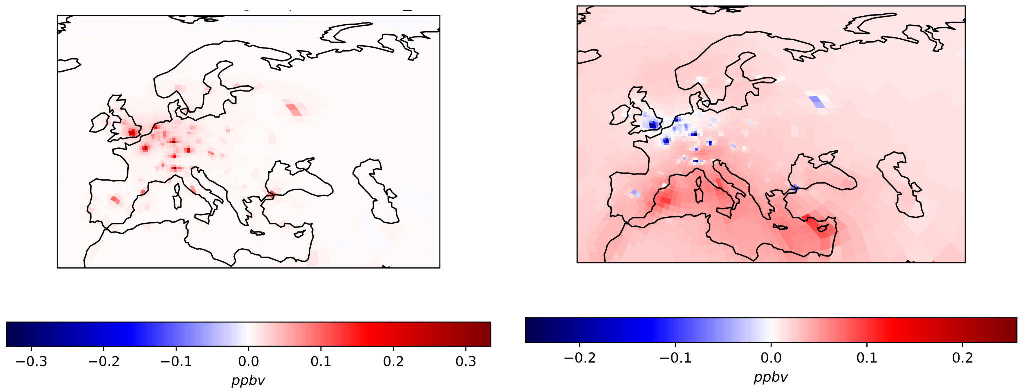

Figure 3.3 - LTO attributable annual-averaged NO_2 (left) and O_3 concentration in Europe in $ppbv$ at surface level.

3.1.5. Next steps

The following step is to repeat the analysis using grids with different refinement levels. A C48 and a C96 stretched grid using the same parameters, i.e., stretch factor, target latitude, and target longitude. The objective is to compare the results produced on each grid, e.g., by comparing population weighted species averages for each resolution or by performing a grid independence test. This step is designed to identify a grid resolution which can provide sufficiently accurate concentration maps and population exposed estimates at a reasonable computational cost.

Once a proper grid resolution has been identified, the investigation of local air quality impacts of aviation in the vicinity of airports will proceed to perform sensitivity analysis with respect to the species of interest for air quality, e.g., $PM_{2.5}$, O_3, NO_X, and BC, with the goal of verifying how an increase/decrease in the emission can increase/decrease local air quality impacts near airports.

Furthermore, the project aims to perform optimisation with the goal of mitigating the impacts of aircraft emissions in local air quality. In order to achieve this, the results from the sensitivity analysis will serve as input for the optimisation with the goal of determining emission values that will minimise air quality impacts.

3.2. Observational approach (S&T)

For the observational approach multiple activities have been done both on the technical side as an investigation into potential end-users for the air quality modelling outputs.

A thorough investigation into the user needs of airports and environmental inspection agencies investigating air quality in proximity of the airports lead to the identification of the following user needs.

Table 3.1 - User needs for air quality monitoring in the vicinity of airports

Description	Source
There is a need for information about local air quality around airports	All interviewed stakeholders
Information about local air quality around airports also needs to be based on measurements, not only on modelling.	Eurocontrol, Antea group
Good spatial coverage of air quality maps is needed to provide more value over the current point measurements.	Environment inspection agency Noordzeekanaalsgebied
Need to monitor the effects of air and car traffic on the health of the residents.	Regional measurement group air and noise pollution SouthEast Brabant
The impact of the blend mandate on local air quality needs to be demonstrated.	Federal office of civil aviation Switzerland
Airports efforts for emission reductions need to be more easily comparable.	European Regions Airline Association
Modelling and measurement efforts need to complement each other for improved air quality insights.	DOI: 10.1021/acs.est.1c03388 10.5194/amt-16-5287-2023
Air quality monitoring for local inspection agencies need better localisation capabilities	Environment inspection agency Noordzeekanaalsgebied
SO_2 monitoring around airports is needed as a measure of Sustainable Aviation Fuel (SAF) acceptance.	SO_2 monitoring around airports is needed as a measure of Sustainable Aviation Fuel (SAF) acceptance.
NO_2 monitoring is needed as the relative contribution of aviation is going up.	European Regions Airline Association

From these user needs the following user requirements have been derived.

Table 3.2 - Derived user requirements for air quality in the vicinity of airports.

Name	Description	Justification
Measurement based	The system shall use local measurements as a basis for the air quality maps	In order to supplement purely modelling based approaches, the system will also include measurements.
Remote sensing based	The system shall use remote sensing measurements as a basis for the air quality maps	In order to supplement purely modelling based approaches, the system will also include measurements. In addition, remote sensing data will allow the user to assess air quality on a larger scale and take background pollution into account.
SAF adaptation	The user shall be able to inspect visualisations of SO2 concentrations around airports throughout multiple years.	Sulphur is relevant for understanding SAF adaptation as aviation is the only industry still having sulphur in their fuels, similar capabilities for the other pollutants are also useful.
Air quality species	The system shall deliver air quality information on the concentration of NO2, SO2, PM2.5 and PM10.	NO2 and SO2 are specifically mentioned by stakeholders, and PM2.5 and PM10 are important to assess overall air quality and contribution of other sources such as road traffic.
Air quality spatial resolution	The system shall deliver maps with a resolution in the order of 100m.	The resolution of the data needs to allow for the identification of the location of pollution sources. Note:

Name	Description	Justification
		Atmospheric Earth Observation data has a resolution of several kilometres, which is not sufficient for our purposes.
Ground level data	The system shall provide concentrations of pollutants at ground level	To study the effect on the local environment, information on ground level is needed.
Consistent mapping	The user should be able to retrieve pollution maps around airports in all EU member states.	Will result in system requirements that ensure data availability
Map size	The system should produce maps of at least 25x25km.	This minimum size is needed to be able to characterise the air quality in the region around the airport and distinguish local pollution from the background.
Time series	The system should produce a time series of data.	Effects of changes in pollution need to be monitored.

To fulfil these requirements, an air quality monitoring system needs to be developed. Currently S[&]T has developed an observational air quality monitoring system, this has been mainly focussed on urban areas and includes NO_2, O_3, PM_{10} and $PM_{2.5}$ pollutants. The Copernicus Atmospheric Monitoring Service (CAMS) is used for retrieving low resolution air quality satellite measurements. This is interpolated onto a ~100m spatial resolution grid aligning with the land use data. The land use is a combination of Urban Atlas and Open Street map data using the main road infrastructure. The next step is to take advection and diffusion effects into account and to apply a correction to the boundary layer height. An update is made to the fit of the land use using ground measurements.

This model is mainly focused on urban air quality. However, airports are often just outside the urban area and the employed land-use maps are not always covering the airports and their proximities. This needs to be adjusted to employ a land-use map that is consistent throughout Europe. For this purpose, two options are under consideration, the Corine land use or ESA's Worldcover dataset supplemented with

Open Street map data. Furthermore, airports and/or air traffic information is not included in the model and the area of interest is likely to be larger than originally used. Therefore some updates to the methodology are necessary to ensure that the observational approach properly takes into account all relevant data sources, is scalable and also includes SO_2 data.

The suggested architecture of the model is shown below. Machine learning plays a key role, creating the base air pollution maps using historical data of land-use, boundary layer height, in-situ sensors, and meteorological data. Different models will be created using a different set of input sources, this is to ensure continuity of the service in case of gaps in input data. At a later stage, the advection and diffusion effects as well as the boundary layer height corrections. The majority of the efforts of the last period have been focussing on the Machine learning model that is an integral part of the new architecture.

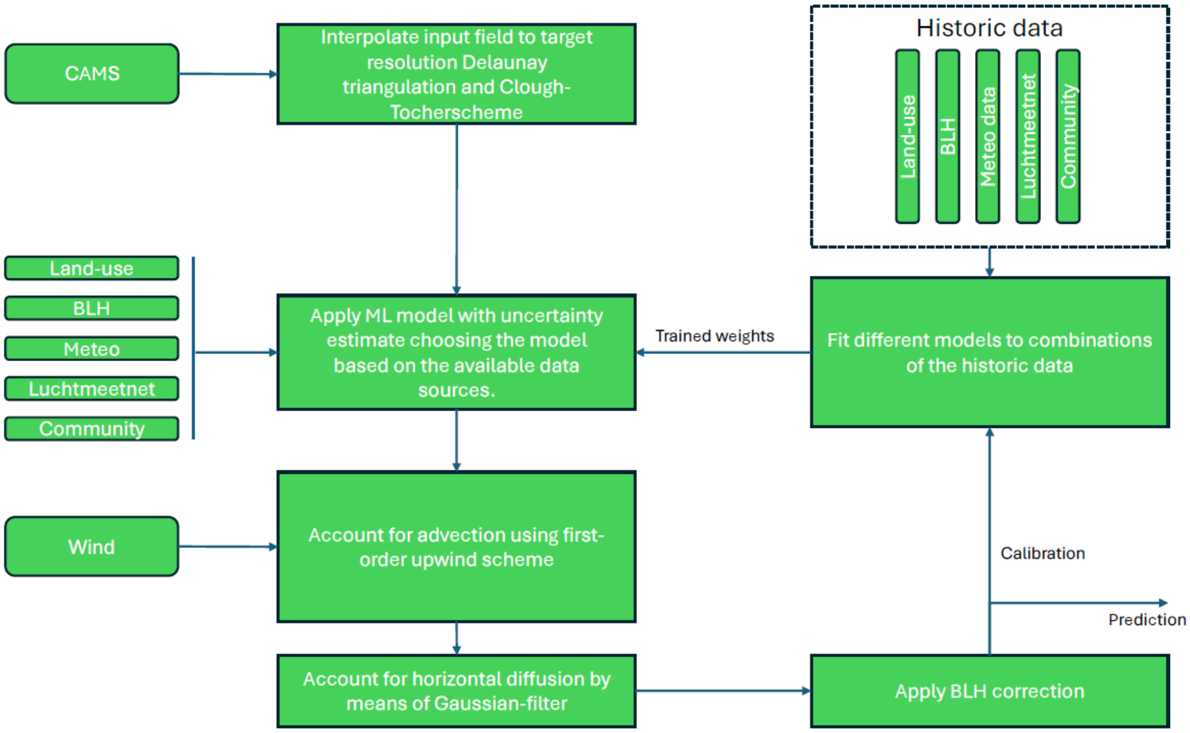

Figure 3.4 - Overview of observational approach for producing air quality maps.

Our Machine Learning framework has been extended to be able to couple datasets with a temporal component as well (previously all use cases required only spatial datasets). Due to the incorporation of the temporal feature, it was necessary to change the sampling of the data to ensure the validity of the data for different input sources. Furthermore, land-use maps have been updated to include more detailed information, especially around airports.

Finally, initial model training has been set up, but is still ongoing. This also includes the definition of the loss functions, which are partly based on CAMS data and partly on the in-situ measurements. This way, the model will learn to adhere to both the satellite data and the in-situ sensors to capture local deviations in pollutant levels. In parallel, a statistical approach is also being pursued, where a generalized linear model is fitted to years of measurements and the same input sources mentioned above.

4. Conclusions

Apart from the University of Birmingham and KTH, most of the results have been developed by each group individually. The research of task T2.5 has reached a degree of maturity that allows for greater interactions between the research groups, and from this point onwards it is expected that more cooperation will take place since the research groups are now in position to produce the results needed by other groups.

References

[1] Holladay, J., Heyne, J., & Abdullah, Z. (2020), *Sustainable Aviation Fuel*, https://www.energy.gov/sites/default/files/2020/09/f78/beto-sust-aviation-fuel-sep-2020.pdf, retrieved 2024-03-12.

[2] Tilson, J., Larkman, J., Plohr, M., Doepellheuer, A., Lischer, T., & Zarzalis, N. (2003), *Future Engine Cycle Prediction and Emissions Study*, AERONET, Deliverable.

[3] Hadaller, O. J., & Johnson, J. M. (2006), *World fuel sampling program*, CRC Report.

[4] Whiteley, M. (2018), *D2.3 European Aviation Fuel Burn and Emissions Inventory System for the European Environment Agency* (for data from 2005), https://www.google.com/url?q=https://www.eurocontrol.int/publication/european-aviation-fuel-burn-and-emissions-inventory-system-feis-european-environment&sa=D&source=docs&ust=1728901582636225&usg=AOvVaw0Qz28YHWV5xRiE_rv-XowX, retrieved 2024-06-11

[5] European Commission - DG CLIMA. (2024), *EU-ETS Reporting tool - User Manual Release version 7.0*, https://www.google.com/url?q=https://climate.ec.europa.eu/document/download/544874bb-9ff6-4fb6-bb55-c4102c0e0aca_en?filename%3DEU-ETS-Reporting%2520-%2520MRV%2520User%2520manual-V15-0.pdf&sa=D&source=docs&ust=1728901582638871&usg=AOvVaw0KnGvY9KdAHQXgpD1QrE_D, retrieved 2024-06-11.

[6] ICAO, *Carbon Offsetting and Reduction Scheme for International Aviation (CORSIA)*, https://www.google.com/url?q=https://www.icao.int/environmental-protection/CORSIA/Pages/default.aspx&sa=D&source=docs&ust=1728901582640715&usg=AOvVaw17SWti7mqAY7_0kYabsdT7, retrieved 2024-06-11.

[7] Leong, C. C., Blakey, S., & Wilson, C. W. (2016), Genetic Algorithm optimised Chemical Reactors network: A novel technique for alternative fuels emission prediction, *Swarm and Evolutionary Computation*, 27, 180–187.

[8] European Union Aviation Safety Agency. (2024), ICAO Aircraft Engine Emissions Databank, https://www.easa.europa.eu/en/domains/environment/icao-aircraft-engine-emissions-databank.

[9] Dooley, S., et al. (2012), The experimental evaluation of a methodology for surrogate fuel formulation to emulate gas phase combustion kinetic phenomena, *Combustion and Flame*, 159(4), 1444–1466, https://doi.org/10.1016/j.combustflame.2011.11.002.

[10] Narayanaswamy, K., Pitsch, H., & Pepiot, P. (2016), A component library framework for deriving kinetic mechanisms for multi-component fuel surrogates: Application for jet fuel surrogates, *Combustion and Flame*, 165, 288–309, https://doi.org/10.1016/j.combustflame.2015.12.013.

[11] Kim, D., Martz, J., & Violi, A. (2014), A surrogate for emulating the physical and chemical properties of conventional jet fuel, *Combustion and Flame*, 161(6), 1489–1498, https://doi.org/10.1016/j.combustflame.2013.12.015.

[12] Yu, W., Tay, K., Zhao, F., Yang, W., Li, H., & Xu, H. (2018), Development of a new jet fuel surrogate and its associated reaction mechanism coupled with a multistep soot model for diesel engine combustion, *Applied Energy*, 228, 42–56, https://doi.org/10.1016/j.apenergy.2018.06.076.

[13] Bhargava, A., Colket, M., Sowa, W., Casleton, K., & Maloney, D. (2000), An Experimental and Modeling Study of Humid Air Premixed Flames, *Journal of Engineering for Gas Turbines and Power*, 122(3), 405–411, https://doi.org/10.1115/1.1286921.

[14] Rutar, T., & Malte, P. C. (2002), NOx Formation in High-Pressure Jet-Stirred Reactors With Significance to Lean-Premixed Combustion Turbines, *Journal of Engineering for Gas Turbines and Power*, 124(4), 776–783, https://doi.org/10.1115/1.1492829.

[15] Brink, L. F. J. (2020), Modeling the impact of fuel composition on aircraft engine NOx, CO, and soot emissions, Massachusetts Institute of Technology, Massachusetts, https://dspace.mit.edu/handle/1721.1/129181.

[16] Lefebvre, A. H., & Ballal, D. R. (2010), *Gas Turbine Combustion* (0 ed.), CRC Press, https://doi.org/10.1201/9781420086058.

[17] Masiol, M., & Harrison, R. M. (2014), Aircraft engine exhaust emissions and other airport-related contributions to ambient air pollution: A review, *Atmospheric Environment*, 95, 409–455, https://doi.org/10.1016/j.atmosenv.2014.05.070.

[18] DuBois, D., & Paynter, G. C. (2006), “Fuel Flow Method2” for Estimating Aircraft Emissions, presented at the Non-Conference Specific Technical Papers - 2006, pp. 2006-01–1987, https://doi.org/10.4271/2006-01-1987.

[19] Ahrens, D., Méry, Y., Guénard, A., & Miake-Lye, R. C. (2023), A New Approach to Estimate Particulate Matter Emissions From Ground Certification Data: The nvPM Mission Emissions Estimation Methodology, *Journal of Engineering for Gas Turbines and Power*, 145(3), 031019, https://doi.org/10.1115/1.4055477.

[20] Fusaro, R., Viola, N., & Galassini, D. (2021), Sustainable Supersonic Fuel Flow Method: An Evolution of the Boeing Fuel Flow Method for Supersonic Aircraft Using Sustainable Aviation Fuels, *Aerospace*, 8(11), 331, https://doi.org/10.3390/aerospace8110331.

[21] Zschocke, A., Scheuermann, S., & Ortner, J. (2012), High Biofuel Blends in Aviation (HBBA): ENER/C2/2012/420-1 Final Report, Deutsche Lufthansa, https://books.google.nl/books?id=HQf6swEACAAJ.

[22] Striebich, R., Shafer, L., Dewitt, M., West, Z., Edwards, T., & Iii, W. (2008), Dependence of Fuel Properties During Blending of Iso-Paraffinic Kerosene and Petroleum-Derived Jet Fuel.

[23] Corporan, E., et al. (2017), Impacts of Fuel Properties on Combustor Performance, Operability and Emissions Characteristics, in *55th AIAA Aerospace Sciences Meeting*, Grapevine, Texas: American Institute of Aeronautics and Astronautics, https://doi.org/10.2514/6.2017-0380.

[24] Beyersdorf, A. J., et al. (2014), Reductions in aircraft particulate emissions due to the use of Fischer–Tropsch fuels, *Atmospheric Chemistry and Physics*, 14(1), 11–23, https://doi.org/10.5194/acp-14-11-2014.

[25] Agarwal, A., et al. (2019), SCOPE11 Method for Estimating Aircraft Black Carbon Mass and Particle Number Emissions, *Environmental Science & Technology*, 53(3), 1364–1373, https://doi.org/10.1021/acs.est.8b04060

[26] Wayson, R. L., Fleming, G. G., & Iovinelli, R. (2009), Methodology to Estimate Particulate Matter Emissions from Certified Commercial Aircraft Engines, *Journal of the Air & Waste Management Association*, 59(1), 91–100, https://doi.org/10.3155/1047-3289.59.1.91.

[27] Teoh, R., et al. (2022), Targeted Use of Sustainable Aviation Fuel to Maximize Climate Benefits, *Environmental Science & Technology*, 56(23), 17246–17255, https://doi.org/10.1021/acs.est.2c05781.

[28] Bulzan, D., et al. (2010), Gaseous and Particulate Emissions Results of the NASA Alternative Aviation Fuel Experiment (AAFEX), in *Volume 2: Combustion, Fuels and Emissions, Parts A and B*, Glasgow, UK: ASMEDC, 1195–1207, https://doi.org/10.1115/GT2010-23524.

[29] Timko, M. T., et al. (2011), Combustion Products of Petroleum Jet Fuel, a Fischer–Tropsch Synthetic Fuel, and a Biomass Fatty Acid Methyl Ester Fuel for a Gas Turbine Engine, *Combustion Science and Technology*, 183(10), 1039–1068, https://doi.org/10.1080/00102202.2011.581717.

[30] Bell, D., Heyne, J. S., Won, S. H., Dryer, F., Haas, F. M., & Dooley, S. (2017), On the Development of General Surrogate Composition Calculations for Chemical and Physical Properties, in *55th AIAA Aerospace Sciences Meeting*, Grapevine, Texas: American Institute of Aeronautics and Astronautics, https://doi.org/10.2514/6.2017-0609.

[31] Vozka, P., Vrtiška, D., Šimáček, P., & Kilaz, G. (2019), Impact of Alternative Fuel Blending Components on Fuel Composition and Properties in Blends with Jet A, *Energy & Fuels*, 33(4), 3275–3289, https://doi.org/10.1021/acs.energyfuels.9b00105.

[32] Airport Air Quality Manual (2020), Doc 9889, *International Civil Aviation Organization*, https://www.icao.int/publications/Documents/9889_cons_en.pdf.

[33] Hunton, D. E., et al. (2000), Chemical ionization mass spectrometric measurements of SO_2 emissions from jet engines in flight and test chamber operations, *Journal of Geophysical Research: Atmospheres*, 105(D22), 26841–26855, https://doi.org/10.1029/2000JD900383.

[34] Quadros, F. D. A., Snellen, M., Sun, J., & Dedoussi, I. (2022), openAVEM (Open Aviation Emissions), *4TU.ResearchData*, https://doi.org/10.4121/15062478.V1.

[35] Quadros, F. D. A., Snellen, M., Sun, J., & Dedoussi, I. C. (2022), Global Civil Aviation Emissions Estimates for 2017–2020 Using ADS-B Data, *Journal of Aircraft*, 59(6), 1394–1405, https://doi.org/10.2514/1.C036763.

[36] Stettler, M. E. J., Eastham, S., & Barrett, S. R. H. (2011), Air quality and public health impacts of UK airports. Part I: Emissions, *Atmospheric Environment*, 45(31), 5415–5424, https://doi.org/10.1016/j.atmosenv.2011.07.012.

[37] Eastham, S. D., et al. (2018), GEOS-Chem High Performance (GCHP v11-02c): a next-generation implementation of the GEOS-Chem chemical transport model for massively parallel applications, *Geoscientific Model Development*, 11(7), 2941–2953, https://doi.org/10.5194/gmd-11-2941-2018.

[38] Bindle, L., et al. (2021), Grid-stretching capability for the GEOS-Chem 13.0.0 atmospheric chemistry model, *Geoscientific Model Development*, 14(10), 5977–5997, https://doi.org/10.5194/gmd-14-5977-2021.

[39] Quadros, F. D. A. (2024), Global impacts of aircraft emissions on air quality and nitrogen deposition, *Delft University of Technology*, https://doi.org/10.4233/UUID:B54561BD-1141-429F-83E3-A94B966C7A07.